Vascular CXCR4 Limits Atherosclerosis by Maintaining Arterial Integrity

Evidence From Mouse and Human Studies

Yvonne Döring, PhD*
Heidi Noels, PhD*
et al

BACKGROUND: The CXCL12/CXCR4 chemokine ligand/receptor axis controls (progenitor) cell homeostasis and trafficking. So far, an atheroprotective role of CXCL12/CXCR4 has only been implied through pharmacological intervention, in particular, because the somatic deletion of the *CXCR4* gene in mice is embryonically lethal. Moreover, cell-specific effects of CXCR4 in the arterial wall and underlying mechanisms remain elusive, prompting us to investigate the relevance of CXCR4 in vascular cell types for atheroprotection.

METHODS: We examined the role of vascular CXCR4 in atherosclerosis and plaque composition by inducing an endothelial cell (BmxCreER^{T2}-driven)–specific or smooth muscle cell (SMC, SmmhcCreER^{T2}- or TaglnCre-driven)–specific deficiency of *CXCR4* in an apolipoprotein E–deficient mouse model. To identify underlying mechanisms for effects of CXCR4, we studied endothelial permeability, intravital leukocyte adhesion, involvement of the Akt/WNT/β-catenin signaling pathway and relevant phosphatases in VE-cadherin expression and function, vascular tone in aortic rings, cholesterol efflux from macrophages, and expression of SMC phenotypic markers. Finally, we analyzed associations of common genetic variants at the *CXCR4* locus with the risk for coronary heart disease, along with *CXCR4* transcript expression in human atherosclerotic plaques.

RESULTS: The cell-specific deletion of *CXCR4* in arterial endothelial cells (n=12–15) or SMCs (n=13–24) markedly increased atherosclerotic lesion formation in hyperlipidemic mice. Endothelial barrier function was promoted by CXCL12/CXCR4, which triggered Akt/WNT/β-catenin signaling to drive VE-cadherin expression and stabilized junctional VE-cadherin complexes through associated phosphatases. Conversely, endothelial *CXCR4* deficiency caused arterial leakage and inflammatory leukocyte recruitment during atherogenesis. In arterial SMCs, CXCR4 sustained normal vascular reactivity and contractile responses, whereas *CXCR4* deficiency favored a synthetic phenotype, the occurrence of macrophage-like SMCs in the lesions, and impaired cholesterol efflux. Regression analyses in humans (n=259 796) identified the C-allele at *rs2322864* within the *CXCR4* locus to be associated with increased risk for coronary heart disease. In line, C/C risk genotype carriers showed reduced CXCR4 expression in carotid artery plaques (n=188), which was furthermore associated with symptomatic disease.

CONCLUSIONS: Our data clearly establish that vascular CXCR4 limits atherosclerosis by maintaining arterial integrity, preserving endothelial barrier function, and a normal contractile SMC phenotype. Enhancing these beneficial functions of arterial CXCR4 by selective modulators might open novel therapeutic options in atherosclerosis.

The full author list is available on page 401.

*Drs Döring and Noels contributed equally to this work.

†Drs van der Vorst and Neideck contributed equally to this work (see page 401).

Correspondence to: Christian Weber, MD, Institute for Cardiovascular Prevention, Ludwig-Maximilians-University Munich, Pettenkoferstr. 8a und 9, D-80336 München, Germany. E-mail chweber@med.lmu.de

Sources of Funding, see page 401

Key Words: atherosclerosis ■ cadherins ■ endothelial cells ■ receptors, CXCR4 ■ permeability ■ smooth muscle cell phenotype ■ WNT signaling pathway

Clinical Perspective

What Is New?

- We show for the first time that the chemokine receptor CXCR4 in vascular cells limits atherosclerosis.
- Mechanistically, the CXCL12/CXCR4 chemokine ligand/receptor axis promotes endothelial barrier function through VE-cadherin expression and the stabilization of junctional VE-cadherin complexes.
- In arterial smooth muscle cells, CXCR4 sustains vascular reactivity responses and a contractile smooth muscle cell phenotype, whereas *CXCR4* deficiency favors the occurrence of macrophage-like smooth muscle cells in atherosclerotic plaques and impairs cholesterol efflux.
- In humans, we identified a common allele variant within the *CXCR4* locus to be associated with reduced CXCR4 expression in carotid artery plaques and increased risk for coronary heart disease.

What Are the Clinical Implications?

- Our data reveal that specifically enhancing the atheroprotective functions of arterial CXCR4 by selective modulators may open novel therapeutic options in atherosclerosis.
- Because systemic approaches to boost CXCR4 function carry a substantial risk of side effects and suboptimal efficacy, eg, due to proatherogenic effects of CXCR4-bearing hematopoietic cells, we envision a regional application of selectively targeted CXCR4 agonists or modulators through peri- or intravascular routes as a novel therapeutic option in atherosclerosis.
- Regional boosting of vascular CXCR4 may be accomplished using polymer- or nanoparticle-based delivery, as exemplified for microR-126-3p, which we previously showed to de-repress CXCR4 activity in endothelial cells.

The chemokine receptor CXCR4 and its cognate ligand CXCL12 are best known for their role in the homing of progenitor cells to the bone marrow and their mobilization to the periphery.[1] Moreover, the importance of CXCR4 and CXCL12 in cell homeostasis, organ development, and vascularization explains why targeted disruption of either gene results in embryonic or perinatal lethality.[2–4] Stress-induced progenitor cell mobilization has been linked to a double-edged role of the CXCL12/CXCR4 axis after arterial injury. Whereas recruitment of angiogenic early outgrowth cells mediated by CXCL12/CXCR4 contributes to vascular regeneration, the mobilization of smooth muscle progenitor cells drives injury-induced neointima formation.[1,5] However, CXCR4 is not only expressed on progenitor cells, but also on endothelial cells (ECs), vascular smooth muscle cells (SMCs), and diverse leukocyte subsets, all of which play a role in neointima formation and in native or diet-induced atherosclerosis.[1,6] For instance, a protective role of endothelial CXCR4 promoting re-endothelialization after endothelial denudation has been revealed during neointima formation.[7] In turn, an atheroprotective role of the CXCL12/CXCR4 axis has been related to the control of neutrophil numbers and activation,[8,9] and microparticle-mediated recruitment of angiogenic cells, as well.[10]

Given that somatic deletion of the *CXCR4* gene in mice is embryonically lethal, the atheroprotective role of CXCR4 has so far been implied by relying on bone marrow chimeras or using pharmacological inhibitors, eg, systemic treatment with a CXCR4 antagonist.[8] Beyond that, vascular cell–specific effects of CXCR4 in the arterial wall and underlying mechanisms have not been elucidated in the context of atherosclerosis. Likewise, genome-wide association studies have validated significant associations between single nucleotide polymorphisms near *CXCL12* as a lead gene in the 10q11 locus and the risk of coronary artery disease and early myocardial infarction,[11,12] whereas a role of CXCR4 variants, in particular, those associated with cardiovascular risk beyond lipid levels,[13] remains unknown.

Here, we examined the role of vascular CXCR4 in atherosclerosis by introducing an EC-specific and SMC-specific deficiency of *Cxcr4* in a mouse model of diet-induced atherosclerosis, identified mechanisms underlying atherosclerosis-related effects of CXCR4 in these cell types, and analyzed the association of common *CXCR4* variants with the risk for coronary heart disease (CHD), and *CXCR4* expression in human atherosclerosis, as well.

METHODS

Please see the online-only Data Supplement for expanded methods.

Animals

All mice were on a C57/Bl6 background (online-only Data Supplement Table I). For atherosclerosis studies, mice were fed a high-fat diet (HFD) containing 21% fat and 0.15% to 0.2% cholesterol (Altromin 132010, Sniff TD88137) for 12 weeks. All animal studies were approved by the local ethical committee.

Lesion Analysis and Intravital Microscopy

For analysis of atherosclerotic lesions, the aortic root and thoracoabdominal aorta were stained for lipid depositions with Oil Red O. Lesions in the root were quantified and averaged in 3 to 5 sections per mouse. Immunohistochemistry was performed to assess cellular composition. Leukocyte adhesion in carotid arteries was investigated by using intravital microscopy.

In Vivo Permeability Assay

Endothelial permeability in the aortic arch was studied using Evans blue (1%, 30 minutes).

Cell Culture

Human aortic endothelial cells (hAoECs, Lonza), SV-40–transformed mouse endothelial cells, and human aortic vascular smooth muscle cells (hAoSMCs, Lonza) were used.

Small Interfering RNA Silencing and Gene Expression Analysis

Specific knock-down of β-catenin and CXCR4 (online-only Data Supplement Table II) in hAoECs was accomplished by application of RNA interference technology (Qiagen). RNA was isolated using RNeasy kits and Tissuelyser (both Qiagen) and reverse transcribed using Moloney murine leukemia virus reverse transcriptase (Promega). Quantitative real-time polymerase chain reaction was performed using the Sybrgreen (online-only Data Supplement Table III). Gene expression was normalized to GAPDH using the ΔΔCt method.

Transcription-Based Reporter Assay

WNT/β-catenin signaling activity was quantified in hAoECs by using a β-catenin–activated reporter system containing multimerized transcription factor/lymphoid enhancer-binding factor DNA-binding sites with inserted Gaussia luciferase as a reporter gene. Conditioned media were analyzed using the Gaussia luciferase assay kit (New England Biolabs) and a plate luminometer (Tecan).

In Vitro Permeability and Scratch Assay

An in vitro permeability assay (Millipore) was performed with hAoEC monolayers grown in 96-well cell culture inserts with a semipermeable membrane using fluorescein isothiocyanate-dextran. A scratch was introduced by dragging a sterile pipette tip across confluent hAoSMC monolayers to create a cell-free path, which was used for monitoring cell migration.

Vascular Reactivity

The thoracic aorta was divided into equal rings. Each aortic ring was connected to a force transducer in organ chambers using a passive tension of 2*g* for subsequent manipulation.

Analysis of CXCR4 in Humans

We examined the association of 345 common variants at the *CXCR4* locus (±25 kB) in association with CHD by using data on altogether 92 516 CHD cases and 167 280 controls (see online-only Data Supplement Table IV for details of data sets included). Human carotid artery endarterectomy specimens (n=218) were collected in a cohort of patients undergoing vascular surgery, and utilization of human vascular tissues was approved by the Ethics Committee of the Medical Faculty at the TU Dresden (EK316122008). Quantification of *CXCR4* mRNA expression and genotyping of rs2322864 in human specimens was performed and correlated with the clinical phenotype.

Statistical Analysis

All data are expressed as mean±SD or mean±standard error of the mean, as indicated. Statistical analyses were performed using GraphPad Prism 6 (GraphPad Software Inc). After testing for normality, unpaired Student *t* test (with Welch correction for mouse studies), Mann-Whitney, 1-way analysis of variance (ANOVA) with the Tukey or Sidak multiple comparisons test, Kruskal-Wallis test with Dunn post test, 2-way ANOVA or 2-way repeated-measures ANOVA with Bonferroni post test were used, as appropriate. *P* values <0.05 were considered statistically significant.

RESULTS

CXCR4 on Arterial ECs Is Atheroprotective

To focus on EC-specific effects of CXCR4 in atherosclerosis-prone mice lacking the *Apoe* gene (*Apoe*$^{-/-}$) and subjected to hyperlipidemia, Cxcr4-floxed (*Cxcr4*$^{fl/fl}$) *Apoe*$^{-/-}$ mice were crossed with *BmxCreER*^{T2}-expressing mice (termed *BmxCre*), mediating efficient tamoxifen-inducible *Cxcr4* deletion in arterial ECs (Figure 1A, online-only Data Supplement Figure IA).[7] After 12 weeks of HFD, *BmxCre*$^{+}$*Cxcr4*$^{fl/fl}$*Apoe*$^{-/-}$ mice displayed larger atherosclerotic lesions in the aortic root (Figure 1B through 1D), the aortic arch (Figure 1E), and the aorta (Figure 1F), in comparison with *BmxCre*$^{-}$*Cxcr4*$^{fl/fl}$*Apoe*$^{-/-}$ controls. Whereas the relative SMC content (Figure 1G) and collagen content (online-only Data Supplement Figure IB) in aortic root lesions were unaltered, macrophage content (Figure 1H and 1I, online-only Data Supplement Figure IC) and the necrotic core area (Figure 1J, online-only Data Supplement Figure ID) were increased in *BmxCre*$^{+}$*Cxcr4*$^{fl/fl}$*Apoe*$^{-/-}$ mice. Conversely, the relative presence of ECs in root lesions was decreased in *BmxCre*$^{+}$ *Cxcr4*$^{fl/fl}$*Apoe*$^{-/-}$ mice (online-only Data Supplement Figure IE and IF). Whereas the density of ECs lining the plaque cap was changed (online-only Data Supplement Figure IG), the number of intercellular adhesion molecule-1–positive cells lining the plaque cap, likely corresponding to activated ECs, was increased (Figure 1K and 1L). This correlated with an increased adhesion of inflammatory monocytes and neutrophils to the carotid artery of tumor necrosis factor α–treated *BmxCre*$^{+}$*Cxcr4*$^{fl/fl}$*Apoe*$^{-/-}$ mice on HFD (Figure 1M and 1N).

The serum levels of CXCL12 (online-only Data Supplement Figure IH), cholesterol, and triglycerides, or body weight did not significantly differ between *BmxCre*$^{-}$ and *BmxCre*$^{+}$*Cxcr4*$^{fl/fl}$*Apoe*$^{-/-}$ mice after HFD (online-only Data Supplement Table V), nor were numbers of leukocytes, neutrophils, monocytes, lymphocytes, and platelets altered in peripheral blood (online-only Data Supplement Figure II, online-only Data Supplement Table V). In the context of arterial injury, EC-specific *Cxcr4* deficiency was found to de-

Circulation. 2017;136:388–403. DOI: 10.1161/CIRCULATIONAHA.117.027646

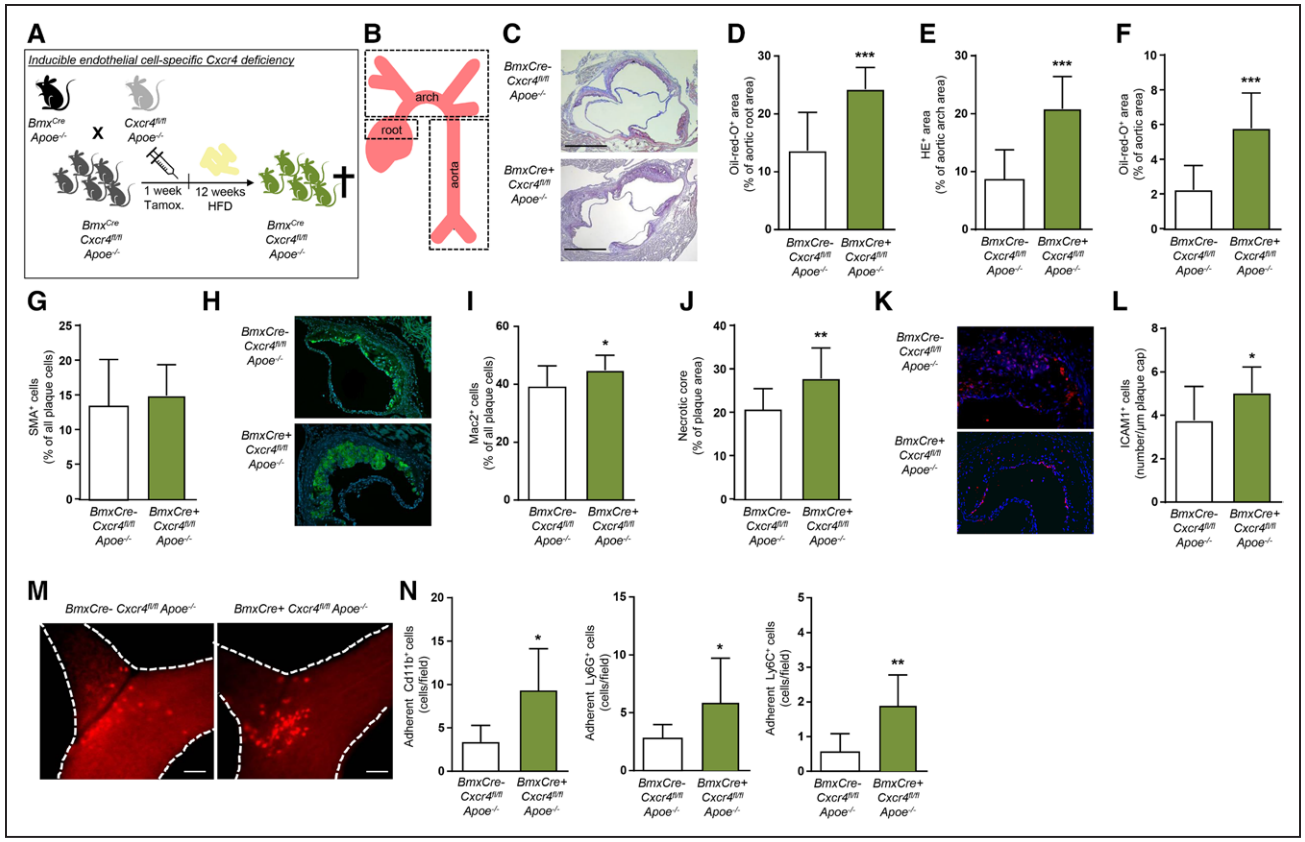

Figure 1. CXCR4 on arterial endothelial cells is atheroprotective.
Cxcr4$^{fl/fl}$*Apoe*$^{-/-}$ mice were crossed with *BmxCreER*^{T2}-expressing mice (termed *BmxCre*), to allow for tamoxifen-inducible *Cxcr4* deletion in arterial endothelial cells. *BmxCre*$^{+}$*Cxcr4*$^{fl/fl}$*Apoe*$^{-/-}$ mice versus *BmxCre*$^{-}$*Cxcr4*$^{fl/fl}$*Apoe*$^{-/-}$ controls were analyzed after 12 weeks of high-fat diet (HFD), unless otherwise indicated. **A** and **B,** Experimental scheme. **C** through **F,** Lesion area measured after Oil Red O or HE staining in the aortic root (**C, D**; n=12–14), aortic arch (**E**; n=12–15)**,** and aorta (**F**; n=12–15). Representative images are shown for aortic root (**C**). Scale bars=500 µm. **G,** SMC content in aortic root lesions, as quantified after staining for SMA (n=12–14). **H** and **I,** Macrophage content in aortic root lesions, as quantified after staining for Mac2 (n=12–14). Representative images are shown in **H**. **J,** Necrotic core area in aortic root lesions, as quantified by anucleated area measurement (n=12–14). **K** and **L,** The number of ICAM-1^{+} cells per micrometer plaque lining in aortic root lesions (n=10–13). Representative images are shown in **K**. **M** and **N,** Representative images (**M**) and quantification (**N**) of intravital microscopy of leukocyte adhesion to TNFα-stimulated carotid arteries of Bmx*Cre*$^{+}$*Cxcr4*$^{fl/fl}$*Apoe*$^{-/-}$ versus *BmxCre*$^{-}$*Cxcr4*$^{fl/fl}$*Apoe*$^{-/-}$ mice after 8 weeks of HFD. Leukocyte labeling was performed for CD11b (all myeloid cells), Ly6G (neutrophils), or Ly6C (monocytes) (n=7–10). **D** through **N,** Data represent mean±SD. **P*<0.05. ***P*<0.01. ****P*<0.001, as analyzed by the Student *t* test with Welch correction or Mann-Whitney test, as appropriate. HE indicates hematoxylin and eosin; ICAM-1, intercellular adhesion molecule-1; SMA, smooth muscle actin; SMC, smooth muscle cell; Tamox., tamoxifen; and TNFα, tumor necrosis factor α.

crease mobilization of Sca1^{+}CD31^{+}Flk1^{+} and Lin^{-}Sca1^{+} progenitor cells,[7] often referred to as circulating angiogenic early-outgrowth cells and SMC progenitors,[5,14] respectively. Because both progenitor subsets have been associated with atheroprotection,[15,16] their mobilization was examined by flow cytometry. No differences in these subpopulations or their CXCR4 expression were observed between *BmxCre*$^{-}$ and *BmxCre*$^{+}$ *Cxcr4*$^{fl/fl}$*Apoe*$^{-/-}$ mice after HFD (online-only Data Supplement Figure IJ through IQ). This indicates that *Bmx* is not expressed in these subsets and thus mainly affects resident arterial ECs. Taken together, our data reveal a proatherogenic effect of endothelial *Cxcr4* deletion, associated with an inflammatory phenotype of the endothelium and increased macrophage content in the atherosclerotic lesions.

CXCR4 on Arterial SMCs Is Atheroprotective

We next examined the contribution of CXCR4 in resident SMCs to atherosclerosis, crossing *Cxcr4*$^{fl/fl}$*Apoe*$^{-/-}$ mice with *TagInCre*-expressing mice for constitutive *Cxcr4* deletion in SMCs[17] (Figure 2A, online-only Data Supplement Figure IIA). In comparison with *TagInCre*$^{-}$ *Cxcr4*$^{fl/fl}$*Apoe*$^{-/-}$ controls, the lesion size in the aortic root (Figure 2B and 2C) and in the aorta (Figure 2D) was significantly increased in *TagInCre*$^{+}$ *Cxcr4*$^{fl/fl}$*Apoe*$^{-/-}$

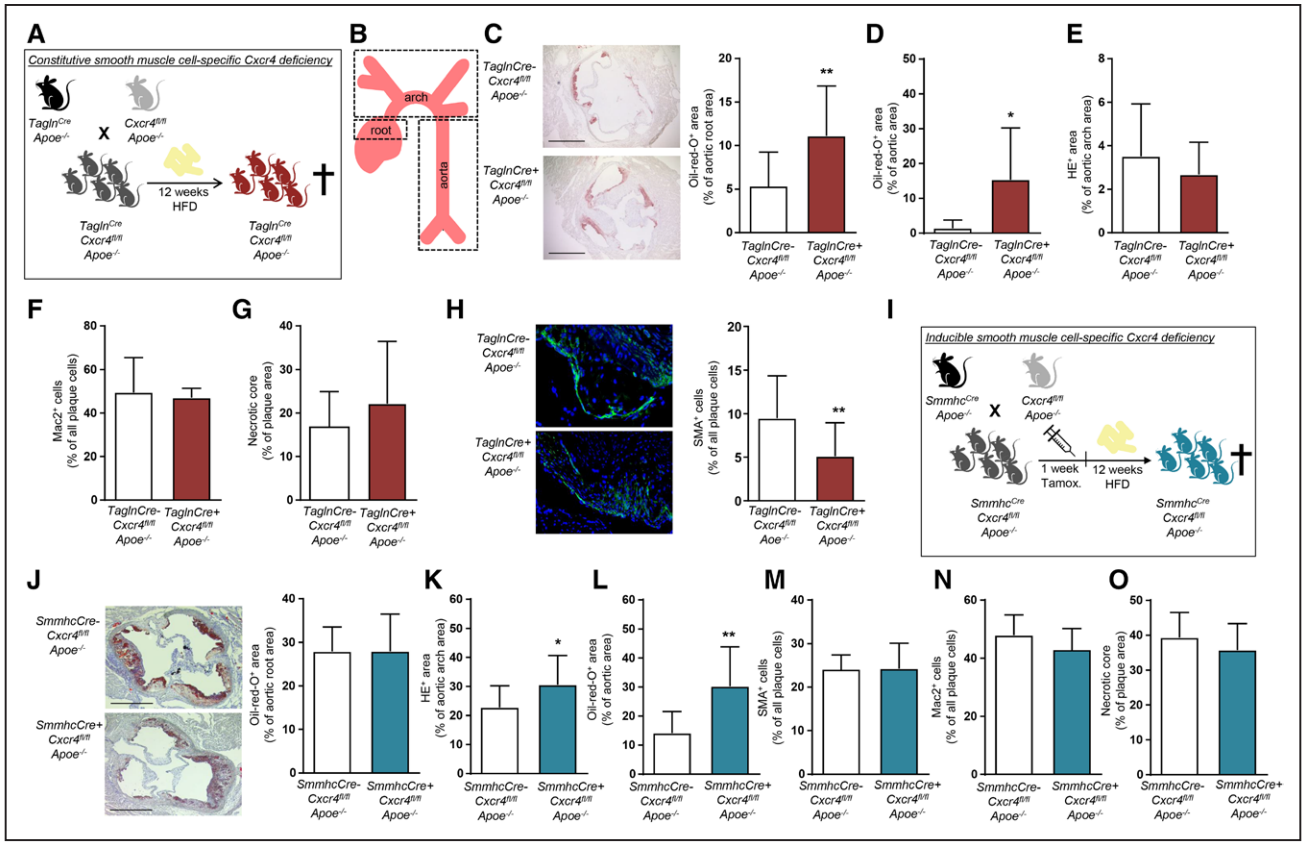

Figure 2. CXCR4 on smooth muscle cells is atheroprotective.
A through **H,** *Cxcr4*$^{fl/fl}$*Apoe*$^{-/-}$ mice were crossed with a *TagInCre*-expressing mouse line, triggering constitutive *Cxcr4* deletion in SMCs. *TagInCre*$^{+}$*Cxcr4*$^{fl/fl}$*Apoe*$^{-/-}$ mice versus *TagInCre*$^{-}$*Cxcr4*$^{fl/fl}$*Apoe*$^{-/-}$ controls were analyzed after 12 weeks of HFD. **A** and **B,** Experimental scheme. **C** through **E,** Lesion area measured after Oil Red O or HE staining in the aortic root (**C**; n=13–24), aorta (**D**; n=6–16), and aortic arch (**E**; n=5–11). Representative pictures are shown for aortic root (**Left**). Scale bars=500 μm. **F,** Macrophage content in aortic root lesions, quantified after Mac2 staining (n=5–16). **G,** Necrotic core area in aortic root lesions, as quantified by anucleated area measurement (n=6–16). **H,** SMC content in aortic root lesions was quantified after staining for SMA and expressed relative to the number of plaque cells (n=13–23). Representative images are shown (**Left**). **I** through **O,** *Cxcr4*$^{fl/fl}$*Apoe*$^{-/-}$ mice were crossed with *SmmhcCreER*^{T2}-expressing mice (termed *SmmhcCre*) to allow for tamoxifen-inducible *Cxcr4* deletion in SMCs. *SmmhcCre*$^{+}$*Cxcr4*$^{fl/fl}$ *Apoe*$^{-/-}$ mice versus *SmmhcCre*$^{-}$*Cxcr4*$^{fl/fl}$*Apoe*$^{-/-}$ controls were analyzed after 12 weeks of HFD. **I,** Experimental scheme. **J** through **O,** Lesional area measured after Oil Red O or HE staining in the aortic root (**J**; n=12–15), aortic arch (**K**; n=10–13), and aorta (**L**; n=12–13). Representative pictures are shown for aortic root (**J**). Scale bars=500 μm. **M** through **O,** Quantification of SMC and macrophage content expressed relative to the number of plaque cells (**M** and **N,** n=12–14) and necrotic core area in aortic root lesions, as quantified by measuring the anucleated area (**O,** n=12–13). (**C** through **O,** Data represent mean±SD. **P*<0.05. ***P*<0.01, as analyzed by Student *t* test with Welch correction or Mann-Whitney test, as appropriate. HE indicates hematoxylin and eosin; HFD, high-fat diet; SMA, smooth muscle actin; and SMC, smooth muscle cell.

mice after 12 weeks of HFD. No differences in plaque size of the aortic arch (Figure 2E) or in lesional macrophage content or necrotic core area of aortic root lesions (Figure 2F and 2G, online-only Data Supplement Figure IIB and IIC) were observed. In contrast, the relative SMC content of aortic root lesions was significantly decreased in *TagInCre*$^{+}$*Cxcr4*$^{fl/fl}$*Apoe*$^{-/-}$ versus *TagInCre*$^{-}$*Cxcr4*$^{fl/fl}$*Apoe*$^{-/-}$ mice (Figure 2H). However, absolute SMC numbers collagen content and the percentage of TUNEL^{+} (terminal deoxynucleotidyl transferase dUTP nick end labeling) cells, indicative of apoptosis, were unaltered (online-only Data Supplement Figure IID through IIF). Whereas leukocyte, neutrophil, monocyte, lymphocyte, and platelet counts in peripheral blood, and CXCL12 serum levels were similar in *TagInCre*$^{-}$ and *TaglCre*$^{+}$ *Cxcr4*$^{fl/fl}$*Apoe*$^{-/-}$ mice (online-only Data Supplement Figure IIG and IIH, online-only Data Supplement Table VI), cholesterol and triglyceride serum levels were lower and body weight was slightly decreased in *TagInCre*$^{+}$*Cxcr4*$^{fl/fl}$*Apoe*$^{-/-}$ mice (online-only Data Supplement Table VI).

As an alternative to constitutive SMC-specific *Cxcr4* deletion, we studied atherosclerosis in *SmmhcCre*$^{+}$ *Cxcr4*$^{fl/fl}$*Apoe*$^{-/-}$ mice (Figure 2I), enabling a tamoxifen-inducible *Cxcr4* deletion in SMCs.[18] Whereas lesion size did not differ in the aortic root (Figure 2J),

a significant increase in lesion size was observed in the aortic arch and in the aorta of *SmmhcCre*$^{+}$*Cxcr4*$^{fl/fl}$*Apoe*$^{-/-}$ mice versus *SmmhcCre*$^{-}$*Cxcr4*$^{fl/fl}$*Apoe*$^{-/-}$ controls after 12 weeks of HFD (Figure 2K and 2L). The lesional content of SMCs and macrophages and the necrotic core area (Figure 2M through 2O, online-only Data Supplement Figure III through IIK) in aortic root lesions were unchanged. No differences in peripheral blood leukocyte and platelet counts, body weight, plasma levels of cholesterol, triglycerides, and CXCL12 were observed between *SmmhcCre*$^{+}$ and *SmmhcCre*$^{-}$*Cxcr4*$^{fl/fl}$*Apoe*$^{-/-}$ mice after HFD (online-only Data Supplement Figure IIL and IIM, online-only Data Supplement Table VII). Furthermore, bone marrow (BM) reconstitution studies revealed that CXCR4 on BM-derived ECs does not affect atherosclerosis, whereas CXCR4 on a subset of BM-derived SMCs is proatherogenic (online-only Data Supplement Figure III, online-only Data Supplement Tables VII and VIII). These effects are apparently unrelated to the function of CXCR4 in resident vascular cells.

Endothelial CXCR4 Reduces Vascular Permeability Through WNT/β-Catenin

To identify the processes underlying the atheroprotective functions of endothelial CXCR4, we examined its role in vascular permeability, which is crucially regulated by the EC layer,[19] also given that increased permeability is associated with enhanced atherosclerosis.[20] Histamine-induced vascular permeability was increased in C57/Bl6 mice pretreated with the CXCR4 antagonist AMD3465 for 16 hours (Figure 3A through 3C), whereas systemic pretreatment with the CXCR4 ligand CXCL12 for 4 hours reduced histamine-induced vascular permeability (Figure 3D). Under conditions of HFD, vascular permeability was increased in *Apoe*$^{-/-}$ mice with an endothelial-specific *Cxcr4* deficiency (Figure 3E through 3G, phosphate-buffered saline–treated group). Similarly, blockade of CXCR4 with AMD increased vascular permeability in *Apoe*$^{-/-}$ mice but did not affect vascular permeability in *BmxCre*$^{+}$ versus *BmxCre*$^{-}$*Cxcr4*$^{fl/fl}$*Apoe*$^{-/-}$ mice (Figure 3F and 3G). In vitro, the permeability of hAoECs, which express CXCR4 on their surface (online-only Data Supplement Figure IVA), to fluorescein isothiocyanate-dextran was increased by activation with the inflammatory cytokine tumor necrosis factor α (online-only Data Supplement Figure IVB). In contrast, permeability was reduced by treatment of hAoECs with CXCL12 for 24 hours and even by short stimulation with CXCL12 for 15 minutes (Figure 3H through 3J). These effects were prevented by the CXCR4 antagonist AMD3100 (Figure 3H through 3J), indicating that a CXCL12/CXCR4-mediated mechanism protects the EC barrier function. Likewise, blockade of Akt kinase signaling downstream of CXCR4 using SH5 prevented the reduction in endothelial permeability by CXCL12 (Figure 3K).

Because WNT signaling has been reported to reduce leakage of the blood-brain barrier[21] and β-catenin is present in endothelium covering human atherosclerotic lesions (online-only Data Supplement Figure IVC), we examined a potential role for WNT/β-catenin in CXCL12-mediated protection of arterial endothelial barrier function using a luciferase reporter assay (Figure 4A). In hAoECs, CXCL12 induced a marked increase in WNT activity, which was inhibited by a CXCR4 antagonist, by small intervening RNA–mediated CXCR4 knock-down or by endo-IWR1 as a specific WNT inhibitor (Figure 4B, online-only Data Supplement Figure IVD). Treatment of hAoECs with CXCL12 upregulated β-catenin transcript levels (online-only Data Supplement Figure IVE). Likewise, CXCL12 increased both cytoplasmic and nuclear β-catenin protein levels, an effect blocked by silencing CXCR4 or by inhibiting WNT signaling with endo-IWR1 (Figure 4C, online-only Data Supplement Figure IVF). Accordingly, transcript expression of the WNT target genes *MT1*, *cyclin-D1*, and *axin-2* was upregulated by CXCL12 (online-only Data Supplement Figure IVG). It is noteworthy that treatment with the WNT protein WNT3a, which triggers β-catenin stabilization by binding to the Frizzled receptor, or with the GSK3 inhibitor LiCl to stimulate WNT signaling reduced endothelial permeability (Figure 4D). The reduction of endothelial permeability induced by CXCL12 treatment for 24 hours or 15 minutes could be reversed by endo-IWR1 (Figure 4E, online-only Data Supplement Figure IVH). Together, our data indicate that CXCL12 improves endothelial barrier function through the WNT pathway.

Endothelial CXCR4 Sustains VE-Cadherin Expression and Function

The adherens junctional protein VE-cadherin is an important contributor to endothelial barrier function.[19] Because CXCL12 regulates E-cadherin expression and localization in migrating epithelial cells,[22] we tested a role of VE-cadherin in the CXCL12/CXCR4-mediated control of endothelial permeability. In hAoECs, CXCL12 increased transcript and protein expression of VE-cadherin (Figure 4F, online-only Data Supplement Figure IVI). This was paralleled by reduced protein levels of VE-cadherin in carotid artery lysates of *BmxCre*$^{+}$*Cxcr4*$^{fl/fl}$*Apoe*$^{-/-}$ mice in comparison with controls (Figure 4G). Of note, inhibiting WNT signaling with endo-IWR1 prevented the upregulation of VE-cadherin mRNA and protein levels by CXCL12 (Figure 4F, online-only Data Supplement Figure IVI), indicating that VE-cadherin expression is increased by the CXCL12/WNT pathway. The VE-cadherin–associated phosphatases SHP2, PTP1B,

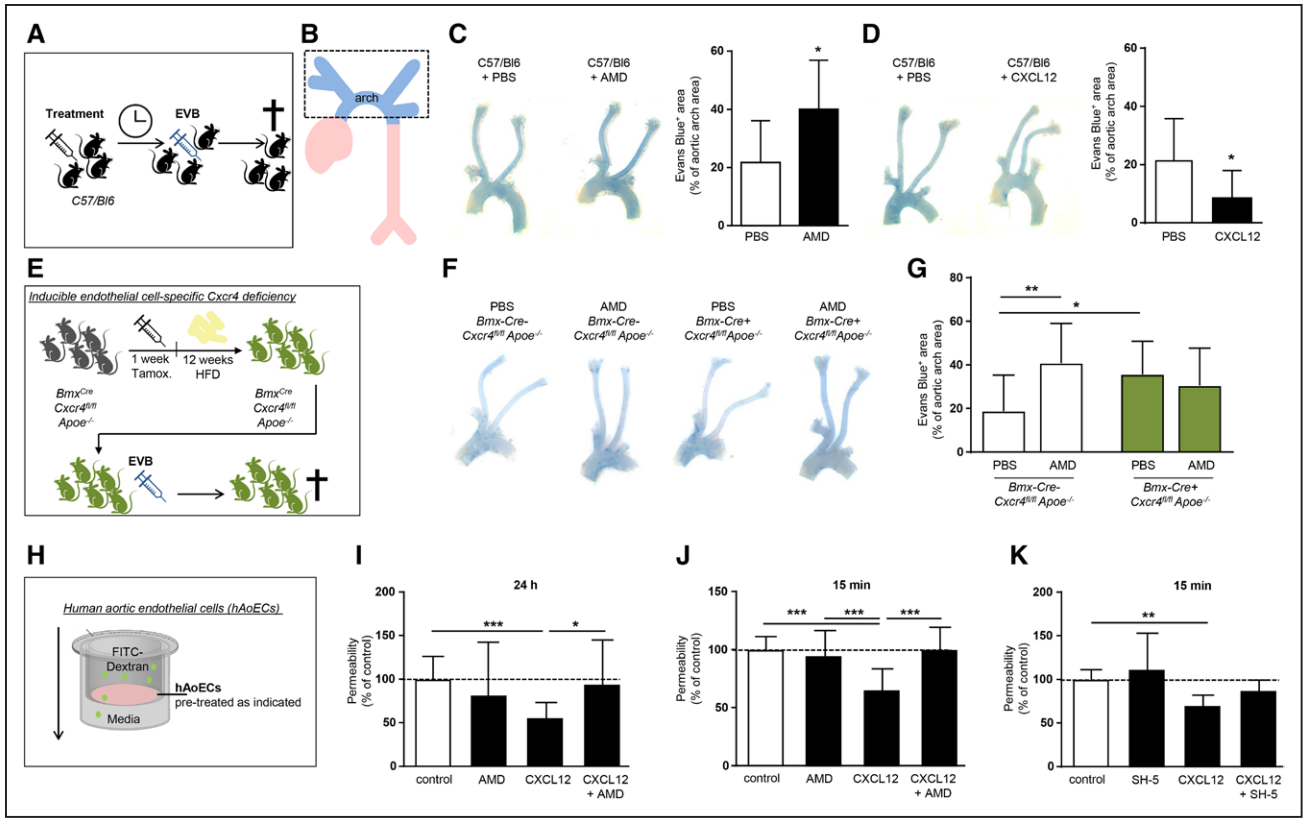

Figure 3. Endothelial CXCR4 reduces vascular permeability through WNT signaling.
A and **B,** Experimental scheme. **C,** Histamine-induced (10 μg IV for 10 minutes) vascular permeability to Evans blue in C57/Bl6 mice pretreated with the CXCR4 antagonist AMD3465 (125 μg/mouse) or vehicle (PBS) for 16 hours, as indicated (n=8–13; Student *t* test with Welch correction). Representative images are shown (**Left**). **D,** Histamine-induced (10 μg histamine IV for 10 minutes) vascular permeability to Evans blue in C57/Bl6 mice pretreated for 4 hours with CXCL12 (3 μg) or vehicle (PBS), as indicated (n=8–13; Student *t* test with Welch correction). Representative images are shown (**Left**). **E,** Experimental scheme. **F** and **G,** Evans blue extravasation in the aortic arch of *BmxCre*$^{-}$*Cxcr4*$^{fl/fl}$*Apoe*$^{-/-}$ and *BmxCre*$^{+}$ *Cxcr4*$^{fl/fl}$*Apoe*$^{-/-}$ mice after 12 weeks of HFD and treated with the CXCR4 antagonist AMD3465 (125 μg/mouse) or vehicle (PBS) for 12 hours, as indicated (n=9–21; 2-way ANOVA with Bonferroni post test). Representative images are shown (**Left**). **H,** Experimental scheme. **I** and **J,** Permeability of hAoECs to FITC-Dextran after stimulation with CXCL12 (100 ng/mL) for 24 hours (**I**) or 15 minutes (**J**). Where indicated, cells were pretreated with the CXCR4 antagonist AMD3100 (**I**) or AMD3465 (**J**) at 1 μg/mL for 1 hour before CXCL12 stimulation. Data in **I** represent n=17 to 20 wells from 7 independent experiments (Kruskal-Wallis test with the Dunn post test). Data in **J** represent n=11 to 19 wells from 6 independent experiments (1-way ANOVA with the Tukey multiple comparisons test). **K,** Permeability of hAoECs to FITC-Dextran after stimulation for 15 minutes with CXCL12 (100 ng/mL) and pretreated with the Akt inhibitor SH-5 (20 nmol/L) for 30 minutes, as indicated (n=6–8 wells from 4 independent experiments; Kruskal-Wallis test with the Dunn post test). **C** through **K**, Graphs represent mean±SD, **P*<0.05. ***P*<0.01. ****P*<0.001. ANOVA indicates analysis of variance; EVB, Evans blue; FITC, fluorescein isothiocyanate; hAoEC, human aortic endothelial cell; HFD, high-fat diet; PBS, phosphate-buffered saline; and Tamox., tamoxifen.

and VE-PTP are known to sustain VE-cadherin function and endothelial barrier integrity.[23,24] Blocking SHP2 and PTPB1 prevented the reduction of endothelial permeability induced by CXCL12 or WNT3a (Figure 4H). Importantly, an increase in histamine-triggered vascular permeability on CXCR4 blockade could not be observed in engineered VE-PTP-FRB^{+}/VE-cadherin-FKBP C57/Bl6 knock-in mice featuring a nondissociating, thus stabilized interaction between VE-cadherin and VE-PTP, which is induced by the chemical compound rapalog and has been previously linked to a preservation of the endothelial barrier[23] (Figure 4I through 4K). Together, our data show that the CXCL12/CXCR4 axis maintains endothelial integrity through the activity of VE-cadherin and VE-cadherin–regulating phosphatases.

CXCL12/CXCR4 signaling did not alter the expression of other tight junctional proteins or inflammatory markers in ECs (data not shown). Finally, because vascular tone regulators such as endothelial nitric oxide synthase have been shown to influence atherogenesis[25] and the EC layer critically regulates vascular tone, we examined a possible role for endothelial CXCR4 in vascular reactivity. No differences were observed in the vascular contraction or relaxation of aortic rings from *BmxCre*$^{+}$

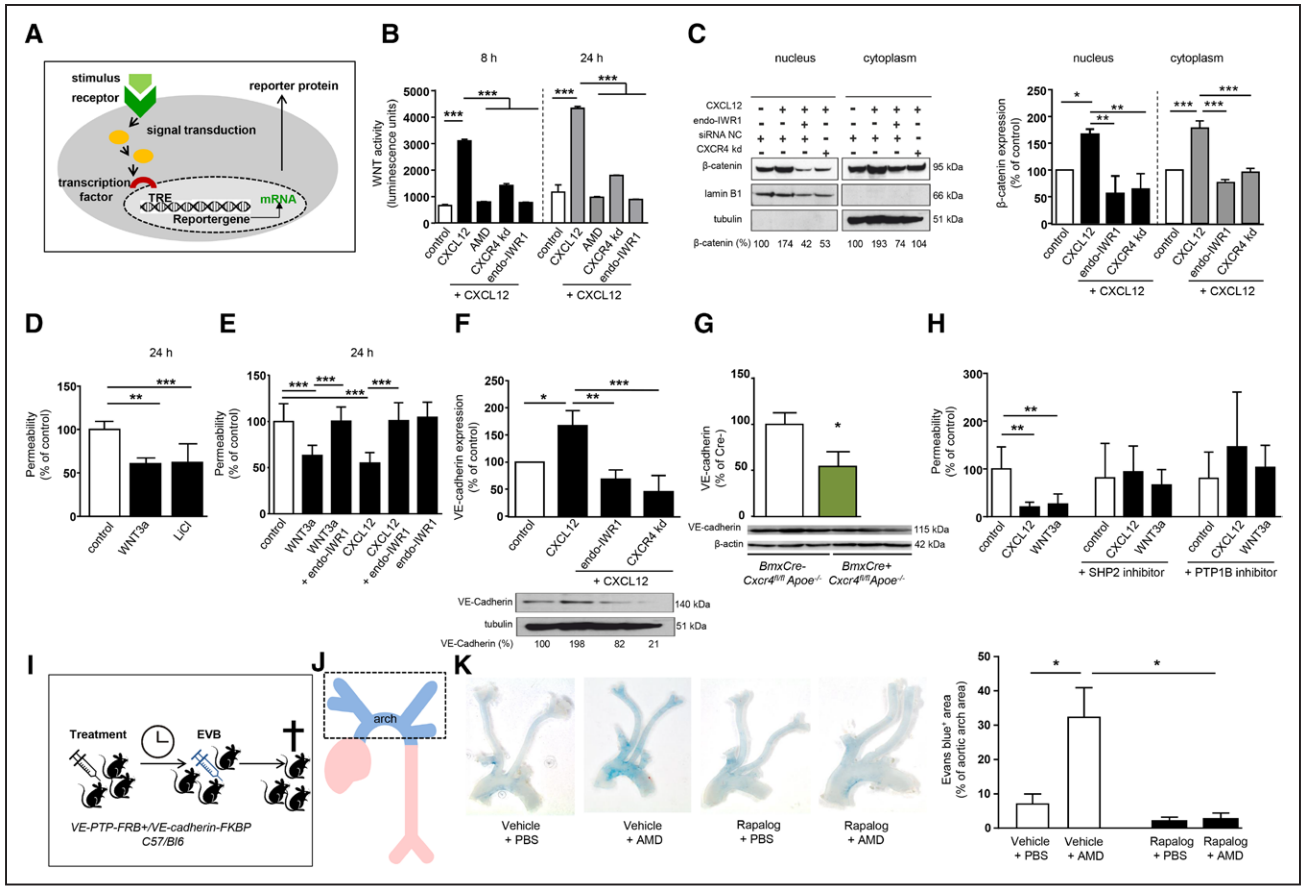

Figure 4. CXCL12/CXCR4 sustains endothelial barrier function through WNT/β-catenin regulating VE-cadherin. **A,** Experimental scheme. **B,** WNT activity in hAoECs as determined in a Gaussia luciferase WNT reporter assay, after stimulation with CXCL12 (100 ng/mL) for indicated periods. Cells were pretreated by the CXCR4 antagonist AMD3100 (1 μg/mL) or *CXCR4* knock-down was performed using siRNA (CXCR4 kd). WNT activation was blocked by the WNT inhibitor endo-IWR1 (10 μmol/L) (n=3; 1-way ANOVA with the Sidak multiple comparisons test). **C,** β-Catenin protein levels in cytoplasmic and nuclear extracts of hAoECs after stimulation with CXCL12 (100 ng/mL) for 24 hours. Cells were pretreated with endo-IWR1 (10 μmol/L). Silencing of CXCR4 was performed using siRNA (CXCR4 kd). β-Catenin levels were normalized to cytoplasmic (tubulin) and nuclear (lamin β1) loading controls, respectively, and presented relative to untreated controls, as quantified by densitometry (n=3; 1-way ANOVA with the Tukey multiple comparisons test). A representative Western blot (**left**) and densitometry quantification (**right**) is shown. **D,** Permeability of hAoECs to FITC-dextran after stimulation with WNT3a (200 ng/mL) or the WNT activator LiCl (30 mmol/L) for 24 hours (n=5–10 wells from 4 independent experiments; Kruskal-Wallis test with the Dunn post test). **E,** Permeability of hAoECs to FITC-dextran after stimulation with WNT3a (200 ng/mL) or CXCL12 (100 ng/mL) for 24 hours and pretreatment with endo-IWR1 (1 μmol/L) for 1 hour, as indicated (n=7–9 wells from 3 independent experiments; 1-way ANOVA with the Tukey multiple comparisons test). **F,** VE-cadherin protein levels in cytoplasmic extracts of hAoECs after stimulation with CXCL12 (100 ng/mL) for 24 hours and treatment with endo-IWR1 (10 μmol/L), as indicated. Knock-down of CXCR4 was performed using siRNA (CXCR4 kd). VE-cadherin expression was normalized to tubulin and presented relative to untreated, as quantified by densitometry (n=3; 1-way ANOVA with the Tukey multiple comparisons test). A representative Western blot and densitometry quantification is shown. Controls received control siRNA (**B, C,** and **F**). **G,** Quantification of VE-cadherin expression in carotid artery lysates of *BmxCre*$^{+}$ versus *BmxCre*$^{-}$*Cxcr4*$^{fl/fl}$*Apoe*$^{-/-}$ mice (n=3; Mann-Whitney test). **H,** Permeability of hAoECs to FITC-dextran after stimulation with CXCL12 (100 ng/mL) or WNT3a (200 ng/mL) for 24 hours and blockade of SHP2 (5 μmol/L) or PTP1B (25 μmol/L) for 1 hour, as indicated (n=8–12 wells from 4 independent experiments; Kruskal-Wallis test with the Dunn post test). **I** through **K,** Vascular permeability to Evans blue induced by histamine (10 μg IV, 10 minutes) in VE-PTP-FRB^{+}/VE-cadherin-FKBP C57/Bl6 knock-in mice pretreated with the CXCR4 antagonist AMD3465 (125 μg) for 12 hours and Rapalog (250 μg) for 4 hours or vehicle, as indicated (n=8–16; 2-way ANOVA with Bonferroni post test). **A** through **K,** Data present mean±SD (**A** through **J**) or mean±SEM (**K**). **P*<0.05. ***P*<0.01. ****P*<0.001. ANOVA indicates analysis of variance; EVB, Evans blue; FITC, fluorescein isothiocyanate; hAoEC, human aortic endothelial cell; PBS, phosphate-buffered saline; and siRNA, small interfering RNA.

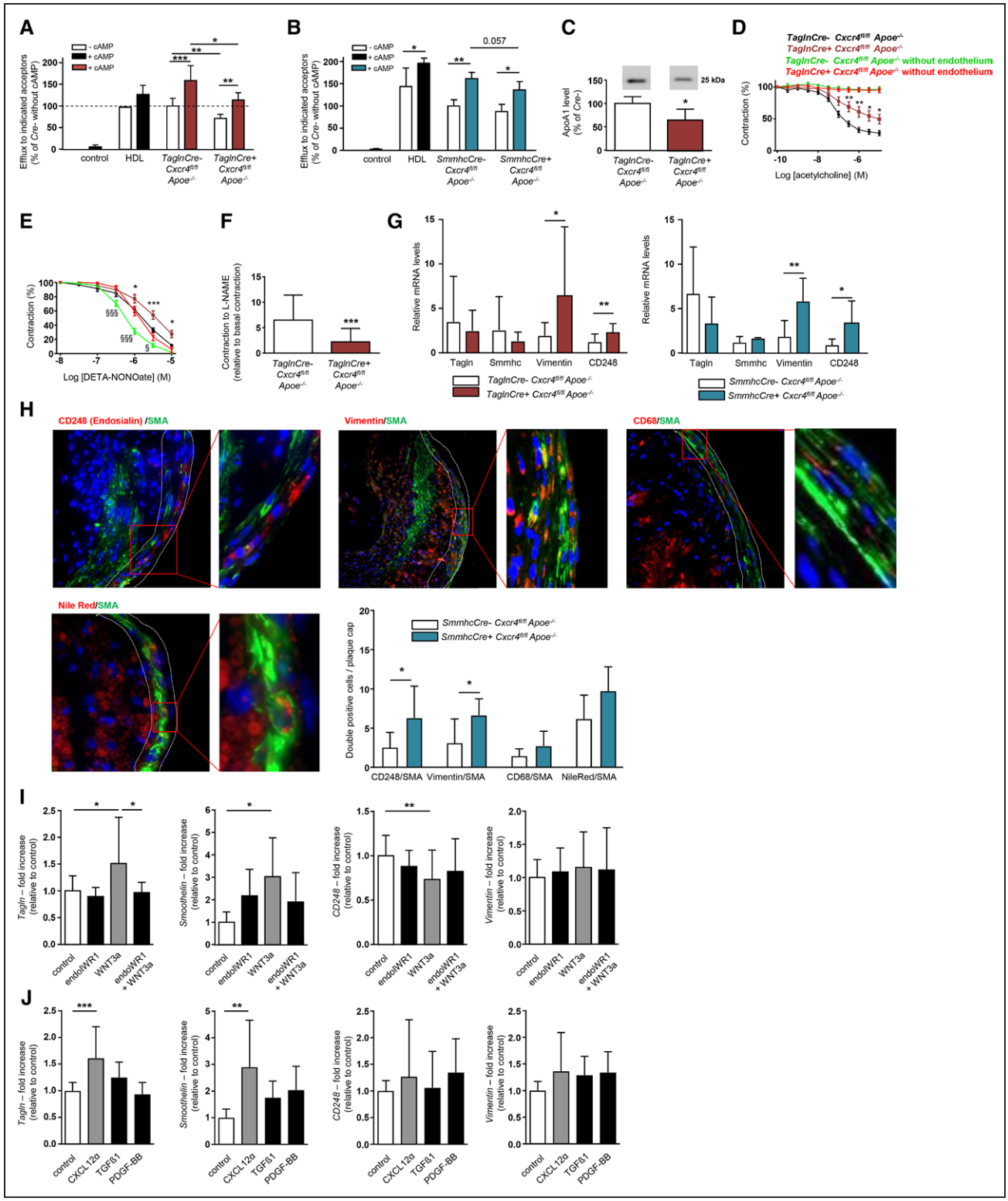

Figure 5. Effect of CXCR4 deletion on cholesterol efflux, vascular tone, and SMC phenotype.
A and **B,** Quantification of cholesterol efflux from lipid-laden macrophages using HDL or pooled serum from *TagInCre*$^{+}$ versus *TagInCre*$^{-}$*Cxcr4*$^{fl/fl}$*Apoe*$^{-/-}$ mice (**A**, n=6) or from *SmmhcCre*$^{+}$ versus *SmmhcCre*$^{-}$*Cxcr4*$^{fl/fl}$*Apoe*$^{-/-}$ mice (**B**, n=4) after 12 weeks of HFD as acceptor. Data represent mean±SD (Mann-Whitney test for comparing Cre^{-} versus Cre^{+}; 2-way ANOVA with Bonferroni post test for comparing without versus with cAMP). **C,** ApoA1 protein levels in serum of *TagInCre*$^{+}$ versus *TagInCre*$^{-}$*Cxcr4*$^{fl/fl}$*Apoe*$^{-/-}$ mice after 12 weeks of HFD, as measured by Western blot analysis. A representative blot and densitometry quantification is shown (n=6; mean±SD; Mann-Whitney test). **D** and **E,** Acetylcholine-induced endothelium-dependent relaxation (**D**, n=20 rings with endothelium or n=9–10 rings without endothelium from 8–9 mice) and (*Continued*)

versus *BmxCre*$^{-}$*Cxcr4*$^{fl/fl}$*Apoe*$^{-/-}$ mice after 12 weeks of HFD or chow diet (online-only Data Supplement Figure VA through VC). Altogether, these data reveal an important function for endothelial CXCR4 in maintaining endothelial barrier integrity via VE-cadherin expression and function, without directly affecting the inflammatory phenotype of ECs or vascular tone.

CXCR4 on SMCs Regulates Lesional Cholesterol Efflux

Cholesterol efflux capacity has been independently and inversely associated with atherosclerotic cardiovascular disease in patients with familial hypercholesterolemia.[26] Analysis of cholesterol efflux revealed a reduction in efflux capacity from lipid-laden macrophages when using serum from *TaglnCre*$^{+}$ versus *TaglnCre*$^{-}$*Cxcr4*$^{fl/fl}$*Apoe*$^{-/-}$ mice on HFD as acceptor. Such reduced cholesterol efflux was observed without and with cAMP stimulation, which enhances cellular lipid efflux to the apolipoprotein acceptor ApoA-1 (Figure 5A).[27] Similar results were obtained by using serum from atherosclerotic *SmmhcCre*$^{+}$ versus *SmmhcCre*$^{-}$*Cxcr4*$^{fl/fl}$*Apoe*$^{-/-}$ mice as acceptor (Figure 5B). Accordingly, serum levels of ApoA-1 were significantly reduced in *TaglnCre*$^{+}$ versus *TaglnCre*$^{-}$*Cxcr4*$^{fl/fl}$*Apoe*$^{-/-}$ mice (Figure 5C). Thus, reduced cholesterol efflux may contribute to increased lipid retention and associated lesion size, as evidenced in *TaglnCre*$^{+}$ and *SmmhcCre*$^{+}$*Cxcr4*$^{fl/fl}$*Apoe*$^{-/-}$ mice (Figure 2).

To identify mechanisms underlying the reduced SMC content in atherosclerotic lesions of *TaglnCre*$^{+}$*Cxcr4*$^{fl/fl}$*Apoe*$^{-/-}$ mice, we analyzed expression of the proliferation marker proliferating cell nuclear antigen in aortic lysates and found lower levels in atherosclerotic aortas of *TaglnCre*$^{+}$*Cxcr4*$^{fl/fl}$*Apoe*$^{-/-}$ mice in comparison with controls after HFD but not a chow diet (online-only Data Supplement Figure VD and VE). Using a scratch assay, we observed an increase in the migratory capacity of hAoSMCs after stimulation with CXCL12, which was inhibited by using a CXCR4 antagonist (online-only Data Supplement Figure VF). Surface expression of CXCR4 on hAoSMCs could be detected by flow cytometric analysis (online-only Data Supplement Figure VG).

CXCR4 on SMCs Supports NO-Dependent Vascular Reactivity

Because SMCs are crucial in regulating vascular tone, we examined the effects of SMC-specific *Cxcr4* deficiency on blood pressure and on vascular contraction and relaxation in organ baths. Systolic and diastolic blood pressure did not differ between *TaglnCre*$^{+}$ versus *TaglnCre*$^{-}$ *Cxcr4*$^{fl/fl}$*Apoe*$^{-/-}$ mice (online-only Data Supplement Figure VH and VI). On treatment with acetylcholine, the relaxation of aortic rings isolated from *TaglnCre*$^{+}$*Cxcr4*$^{fl/fl}$*Apoe*$^{-/-}$ mice after HFD for 12 weeks was impaired in comparison with those from *TaglnCre*$^{-}$*Cxcr4*$^{fl/fl}$*Apoe*$^{-/-}$ controls (Figure 5D). Acetylcholine induces nitric oxide (NO) production in ECs to trigger SMC relaxation, explaining the unresponsiveness of aortic rings lacking the EC layer (Figure 5D). Reduced relaxation capacity of *TaglnCre*$^{+}$*Cxcr4*$^{fl/fl}$*Apoe*$^{-/-}$ aortic rings was also recorded after treatment with the NO donor (Z)-1-[2-(2-aminoethyl)-N-(2-ammonioethyl)

Figure 5 Continued. DETA-NONOate–induced endothelium-independent relaxation (**E**, n=16–18 rings with endothelium or n=11–16 rings without endothelium from 8–9 mice) of aortic rings from *TaglnCre*$^{+}$ versus *TaglnCre*$^{-}$*Cxcr4*$^{fl/fl}$*Apoe*$^{-/-}$ mice after 12 weeks of HFD, with or without removal of the endothelium, as indicated. Data represent mean±SEM (2-way repeated-measures ANOVA with Bonferroni post test for comparing *Cre*$^{-}$ versus *Cre*$^{+}$). **F,** Ratio of L-NAME-induced contraction (300 μmol/L L-NAME) to basal precontraction without L-NAME in aortic rings from *TaglnCre*$^{+}$ versus *TaglnCre*$^{-}$*Cxcr4*$^{fl/fl}$*Apoe*$^{-/-}$ mice after 12 weeks of HFD (n=20–21 rings from 8–9 mice). Data represent mean±SEM (Mann-Whitney test). **G,** Relative quantification of *transgrelin* (*Tagln*), *smooth muscle-myosin heavy chain* (*Smmhc*), *vimentin* and *CD248* (*endosialin*) mRNA expression in thoracic aortas of *TaglnCre*$^{+}$ versus *TaglnCre*$^{-}$*Cxcr4*$^{fl/fl}$*Apoe*$^{-/-}$ and *SmmhcCre*$^{+}$ versus *SmmhcCre*$^{-}$*Cxcr4*$^{fl/fl}$*Apoe*$^{-/-}$ mice after normalization to *18S* rRNA (n=3–9). Data represent mean±SD, Student *t* test with Welch correction or Mann-Whitney test, as appropriate. **H,** Representative images and quantification of protein expression of CD248 (endosialin), vimentin, and CD68, and lipid deposition (Nile red) in atherosclerotic lesions (plaque cap) in mice with SMC-specific *Cxcr4* deficiency, in comparison with controls (n=6–10). Data represent mean±SD and were analyzed by the Student *t* test with Welch correction or Mann-Whitney test, as appropriate (**G** and **H**). **I,** Relative quantification of *Tagln, smoothelin, CD248*, and *vimentin* mRNA expression in hAoSMCs, pretreated with endoIWR1 (1 μmol/L) and stimulated with WNT3a (200 ng/mL), as indicated. Data are normalized to *Gapdh* expression (mean±SD, data combined from 3–7 experiments, each performed in triplicate; 1-way ANOVA with the Sidak multiple comparisons test or Kruskal-Wallis test with the Dunn multiple comparisons test, as appropriate). **J,** Relative quantification of *Tagln, smoothelin, CD248*, and *vimentin* mRNA expression in hAoSMCs stimulated with (protease-resistant) CXCL12 (100–300 ng/mL), TGF-β (2.5 ng/mL), or PDGF-BB (20 ng/mL) as indicated. Data are normalized to *Gapdh* expression (mean±SD, data combined from 3–5 experiments, each performed in triplicate; 1-way ANOVA with the Sidak multiple comparison test or Kruskal-Wallis test with the Dunn multiple comparison test, as appropriate). **A** through **J,** **P*<0.05. ***P*<0.01. ****P*<0.001. ANOVA indicates analysis of variance; DETA-NONOate, (Z)-1-[2-(2-aminoethyl)-N-(2-ammonioethyl)amino]diazen-1-ium-1,2-diolate; hAoSMC, human aortic vascular smooth muscle cell; HDL, high-density lipoprotein; HFD, high-fat diet; L-NAME, N$^{\omega}$-nitro-L-arginine methyl ester; PDGF, platelet-derived growth factor; SEM, standard error of the mean; SMA, smooth muscle actin; SMC, smooth muscle cell; and TGF-β, transforming growth factor β.

amino]diazen-1-ium-1,2-diolate triggering EC-independent relaxation (Figure 5E). A comparable reduction in (Z)-1-[2-(2-aminoethyl)-N-(2-ammonioethyl)amino] diazen-1-ium-1,2-diolate–induced relaxation was observed in the absence of the EC layer (Figure 5E). Moreover, contraction triggered by the NO synthase inhibitor N^{ω}-nitro-L-arginine methyl ester was lower in aortic rings from *TaglnCre*$^{+}$*Cxcr4*$^{fl/fl}$ *Apoe*$^{-/-}$ mice versus controls after HFD (Figure 5F). Similar results were obtained in rings from mice receiving a chow diet (online-only Data Supplement Figure VJ and VL). Of note, plasma levels of NO did not differ between genotypes on chow or HFD (online-only Data Supplement Figure VM and VN). This indicates that the impairment in vascular reactivity of *TaglnCre*$^{+}$*Cxcr4*$^{fl/fl}$*Apoe*$^{-/-}$ aortic rings was attributable to reduced responsiveness of SMCs rather than to reduced NO availability. By comparison, tamoxifen-induced *SmmhcCre*-driven deletion of *Cxcr4* resulted in a less pronounced impairment in (Z)-1-[2-(2-aminoethyl)-N-(2-ammonioethyl)amino] diazen-1-ium-1,2-diolate–induced vascular relaxation in *SmmhcCre*$^{+}$ versus *SmmhcCre*$^{-}$*Cxcr4*$^{fl/fl}$*Apoe*$^{-/-}$ mice but did not affect acetylcholine-induced relaxation or N^{ω}-nitro-L-arginine methyl ester–induced contraction (online-only Data Supplement Figure VO through VQ). Collectively, our data indicate that *Cxcr4* deficiency in SMCs exerts rather moderate effects on vascular tone per se and that the more marked impairment observed in *TaglnCre*$^{+}$*Cxcr4*$^{fl/fl}$*Apoe*$^{-/-}$ mice is likely attributable to the constitutive *Cxcr4* deficiency during vascular development.

CXCR4 Maintains SMCs in a Contractile Phenotype

Vascular SMCs display a significant plasticity and can dedifferentiate from a contractile phenotype to a more synthetic phenotype. This SMC phenotype switching has recently been implicated in influencing atherosclerosis.[28] We found that mice with SMC-specific *Cxcr4* deficiency showed an increased aortic expression of vimentin, a synthetic marker induced by platelet-derived growth factor BB,[29] and of CD248 (endosialin), which is involved in platelet-derived growth factor–mediated cellular effects and associated with a synthetic SMC phenotype (Figure 5G, online-only Data Supplement Figure VR and VS).[30,31] Moreover, staining for vimentin, CD248, CD68, and lipids (Nile red) revealed a higher prevalence of dedifferentiated SMCs in plaque caps of these mice (Figure 5H). In vitro, both WNT3a and CXCL12 increased the expression of contractile markers (*Tagln, smoothelin, CNN1*) in cultured hAoSMCs, whereas the expression of synthetic markers was reduced (for CD248 after WNT3A treatment, Figure 5I, online-only Data Supplement Figure VT) or not altered (after CXCL12 treatment, Figure 5J, online-only Data Supplement Figure VU), respectively. Combined with our finding that the CXCL12/CXCR4 axis drives WNT activation (Figure 4B), these data reveal that the CXCL12/CXCR4/WNT axis supports a contractile phenotype in SMCs.

CXCR4 Risk Variants Are Associated With Impaired CXCR4 Expression

We evaluated the relevance of our findings indicating a protective role of CXCR4 to human atherosclerosis. Immunohistochemistry in carotid endarterectomy specimen detected CXCR4 protein expression in both ECs and SMCs of human atherosclerotic lesions (Figure 6A), and the presence of active β-catenin indicating an activation of the WNT pathway, as well (Figure 6B). We next examined the association of all common variants at the *CXCR4* locus with coronary heart disease (CHD) using data on altogether 92 516 CHD cases and 167 280 controls (including CARDIoGRAMplusC4D [Coronary Artery Disease Genome Wide Replication and Meta-analysis Plus the Coronary Artery Disease Genetics]) and fine mapping of data from the 1000 Genomes Project (see online-only Data Supplement Table IX for details of data sets included). Thus, we identified the C-allele at rs2322864 (minor allele frequency 26%) to be significantly associated with increased CHD risk (odds ratio, 1.04 for every C-allele; P=4.38×10^{-7}) (Figure 6C) and with reduced *CXCR4* gene expression in whole-blood on expressive quantitative trait loci analysis (data not shown). It is noteworthy the C/C-genotype at rs2322864 was found to be linked to reduced *CXCR4* mRNA expression in atherosclerotic plaques of human carotid arteries (Figure 6D). Moreover, *CXCR4* expression was lower in patients with symptomatic versus asymptomatic carotid stenosis, as evident by neurological events, eg, transient ischemic attacks (Figure 6E), consistent with the notion that low vascular CXCR4 levels give rise to increased risk for carotid and coronary atherosclerosis.

DISCUSSION

Our data unequivocally reveal that CXCR4 is atheroprotective in vascular cells by sustaining endothelial integrity and promoting the contractile phenotype of SMCs. This conclusion is supported by the increase in atherosclerosis on arterial EC or SMC-specific deletion of *Cxcr4* in mice, and reduced *CXCR4* expression in human carriers of a common CXCR4 risk variant for CHD, as well. Our results corroborate and extend the importance of CXCR4 in atherosclerosis and human disease beyond previous findings using its systemic blockade or disruption in bone marrow, and its role in stem and cancer cell migration, as well.

Sustained endothelial integrity on CXCL12/CXCR4 signaling was mediated by (1) Akt/WNT signaling, (2)

Circulation. 2017;136:388–403. DOI: 10.1161/CIRCULATIONAHA.117.027646

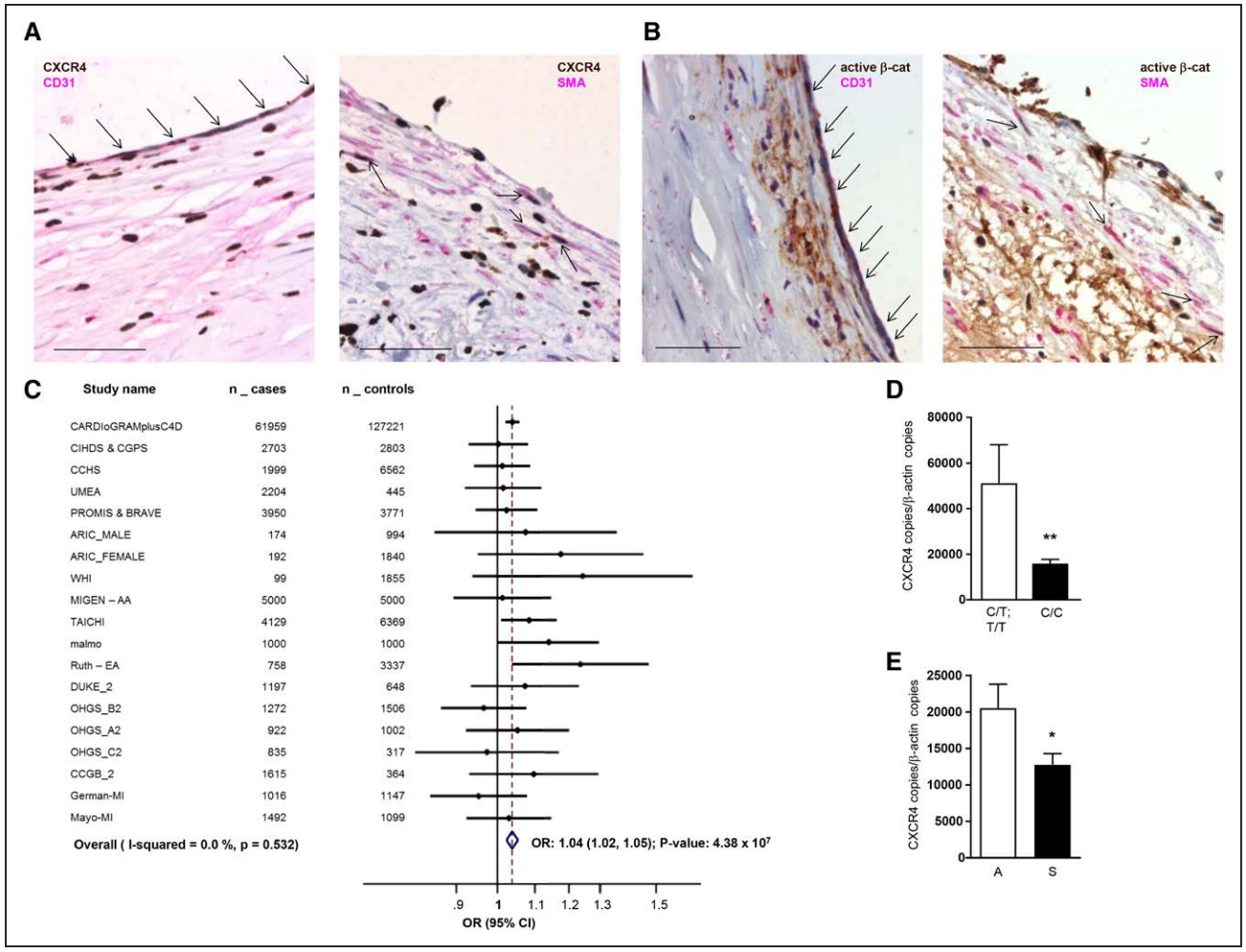

Figure 6. Relevance of CXCR4 pathway expression to human atherosclerotic disease.
A, Staining of CXCR4 in human atherosclerotic lesions. Human carotid endarterectomy specimens were stained for CXCR4 (brown) in combination with CD31 (**Left**, pink) or SMA (**Right**, pink). Scale bar=50 μm. Arrows indicate CXCR4⁺ ECs (**Left**) or CXCR4⁺ SMCs (**Right**). **B,** Staining for active β-catenin in human atherosclerotic lesions. Human carotid endarterectomy specimens were stained for active β-catenin (ABC; brown) in combination with CD31 (**Left**, pink) or SMA (**Right**, pink). Scale bar=50 μm. Arrows indicate ABC⁺ ECs (**Left**) or ABC⁺ SMCs (**Right**). **C**, Forest plot for the associations of CHD risk with *rs2322864*. We examined the association of 345 common variants at the CXCR4 locus (±25 kB) with CHD by using data on 92 516 CHD cases and 167 280 controls (see online-only Data Supplement Table IV for details of data sets included), most notably interrogating the CARDIoGRAMplusC4D data. We conducted fine-mapping studies in 12 500 myocardial infarction cases and 12 000 controls and genotyped all 512 variants with a minor allele frequency >0.1% identified by the 1000 Genomes Project at the *CXCR4* locus. A *P* value of 5×10^{-5} was considered as statistically significant based on Bonferroni correction for 857 variants. Odds ratios (OR) with 95% confidence intervals (CIs) and *P* values are given. The C-allele at *rs2322864* was found to be associated with increased CHD risk (OR, 1.04; $P=4.38\times10^{-7}$). **D**, Association of *rs2322864* with *CXCR4* expression in carotid endarterectomy specimen (C/T; T/T: n=121 and C/C: n=67, Mann-Whitney test with Bonferroni correction to adjust for multiple comparisons). **E,** Correlation of *CXCR4* expression with clinical carotid stenosis, as evident by neurological events, eg, transient ischemic attacks (A, asymptomatic, n=25; S, symptomatic, n=19, unpaired *t* test with Welch correction); *CXCR4* expression was normalized to *β-actin* expression (mean±SEM). **P*<0.05. CHD indicates coronary heart disease; EC, endothelial cell; SEM, standard error of the mean; SMA, smooth muscle actin; and SMC, smooth muscle cell.

involved the VE-cadherin–associating phosphatases VE-PTP, SHP2, and PTP1B,[23,32–34] and was linked with (3) increased VE-cadherin expression and function, as evidenced by reinforced interactions of VE-cadherin and VE-PTP to conserve endothelial barrier function.[23] As a result, interference with the CXCL12/CXCR4 axis enhanced Evans blue extravasation into the vascular wall under conditions of acute inflammation and during atherogenesis in vivo. Moreover, endothelial *Cxcr4* deficiency was associated with an upregulation of intercellular adhesion molecule-1 expression in arterial ECs covering atherosclerotic lesions, reflecting their activation, and promoting atherogenic leukocyte recruitment and increased macrophage content in the lesions. The

latter effect was not attributable to a direct effect of the CXCL12/CXCR4 axis on the expression of inflammatory mediators and adhesion molecules in ECs, because it could not be stimulated or modulated by CXCL12 in vitro. This implies that the marked leukocyte trafficking into early lesions of mice lacking endothelial *Cxcr4* was rather related to disturbed endothelial integrity and increased permeability, subsequently enhancing vascular inflammation and adhesion molecule expression on the endothelium.

WNT activation was previously found to decrease leakage of the blood-brain barrier,[21] implicating β-catenin transcriptional activity in reduced permeability of brain ECs.[35] A link between CXCL12 and WNT has been suggested in peripheral nerve sheath tumors and pancreatic β-cells, triggering cell growth and survival, respectively.[36,37] We found that the CXCL12/CXCR4 axis reduces endothelial permeability through Akt/WNT– and VE-cadherin–mediated mechanisms, which may refine and underlie findings that CXCL12 or its analogs can reduce thrombin-induced endothelial permeability and pulmonary vascular leakage in a model of lipopolysaccharide-induced acute respiratory distress syndrome.[38,39] Notably extending previous findings,[23] stabilizing the interaction between VE-cadherin and VE-PTP prevented the impairment of endothelial barrier function on interference with CXCR4. Surprisingly, atherosclerosis-prone endothelium displays increased β-catenin nuclear localization.[40] However, enhancing WNT signaling by blocking the endogenous β-catenin/WNT inhibitor GSK3 reduced atherosclerosis and inflammatory endothelial VCAM-1 expression,[41] further supporting an atheroprotective role of WNT, at least in part, at the endothelial level. Findings that endothelial KLF4 is itself a β-catenin target gene,[42] drives VE-cadherin expression[43] and is atheroprotective in ECs,[44] may provide additional evidence for a downstream link of CXCL12-induced β-catenin and VE-cadherin expression. Given the involvement of SHP2 in Akt signaling,[45] our data unveil that the CXCL12-CXCR4 axis can sustain endothelial integrity through (1) SHP2/Akt/WNT signaling inducing VE-cadherin expression, and (2) VE-cadherin–associated phosphatases, namely, VE-PTP, supporting VE-cadherin stability and function.

In the second line of investigation, we show that the CXCL12/CXCR4 axis also favors a contractile over a synthetic phenotype in arterial SMCs to explain increased lesion formation in mice with SMC-specific *Cxcr4* deficiency. Phenotype switching of contractile SMCs to a synthetic phenotype has long been considered to contribute to atherogenesis by generating a more inflammatory SMC phenotype.[28] A recent study supported this notion by documenting that loss of myocardin, a promotor of the contractile and noninflammatory SMC phenotype, increased atherosclerosis.[46] Here, we uncover a role for a chemokine ligand/receptor axis in influencing SMC phenotype in the context of atherosclerosis. In addition to upregulating markers (vimentin and endosialin) associated with the synthetic SMC phenotype,[29–31] SMC *Cxcr4* deficiency increasingly switched SMCs in atherosclerotic lesions to a macrophage-like phenotype featuring costaining for CD68 and Nile red. Such SMC-derived macrophage-like cells have only recently been identified in atherosclerotic lesions, and are suggested to augment atherosclerosis.[28,47,48] Likewise, endosialin has been found to promote atherosclerosis through phenotypic remodeling of vascular SMCs.[31] In accord with CXCL12 driving WNT signaling, we confirmed that both CXCL12 and WNT3a promoted the contractile phenotype of SMCs in vitro,[49] consistent with our observations on *Cxcr4* deficiency in vivo. Combined with a reduced macrophage cholesterol efflux capacity attributable to lower ApoA1 serum levels, this may underlie atherogenic effects of *Cxcr4* deficiency in SMCs. It is notable that because an autocrine loop for CXCR4-dependent expression of CXCL12 has been established in ECs,[10] a cross talk of CXCR4-bearing SMCs and ECs via CXCL12 in the arterial wall may also contribute to atheroprotection. Proatherogenic effects of CXCR4 in BM-derived SMCs contrasted a protective role in resident SMCs, likely because of differential expression levels or functions depending on the cellular context and origin.

Genome-wide association studies have validated highly significant associations of variants near *CXCL12* as a lead gene in the 10q11 locus with the risk for CAD and myocardial infarction.[11,12] Based on a more recent analysis, we have now extended the role of CXCL12 to the locus of its receptor CXCR4, showing that a common variant, the C-allele at rs2322864 was associated with increased risk for CHD, and the C/C-genotype was associated with reduced *CXCR4* expression in whole blood and carotid atherosclerotic plaques. Of note, the odds ratio for CHD risk appeared to be more prominent in predominantly female cohorts. *CXCR4* expression was also reduced in patients with symptomatic in comparison with asymptomatic carotid atherosclerosis, indicative of a more unstable plaque phenotype. Collectively, our data substantiate the protective role of the CXCL12/CXCR4 axis in cells of the arterial wall. Because global inducible *Cxcr4* deficiency less markedly exacerbates atherosclerosis (D. Saleheen et al, unpublished data, 2017), CXCR4 may also confer proatherogenic effects in other cell types distinct from neutrophils, ECs, or SMCs; however, the identity of this cell type, eg, in the hematopoietic or other nonvascular cell compartments, remains to be elucidated. Our data linking variants in the *CXCR4* gene locus with CHD risk support the notion that CXCR4 is a disease-modifying receptor in atherosclerosis, indicating that protective effects may prevail, but cannot explain differences or resolve the

directionality in BM-related versus peripheral effects of CXCR4 on atherogenesis.

Our data indicate that specifically enhancing the atheroprotective functions of CXCR4 in different arterial cell types (but not in hematopoietic cells) might open new and exciting therapeutic options. Owing to interference with the role of CXCR4 in progenitor cell mobilization and trafficking, systemic approaches, eg, using noncleavable CXCL12 peptides[39] or small-molecule agonists to boost CXCR4 function, carry a substantial risk of side effects and suboptimal efficacy, eg, attributable to proatherogenic effects of CXCR4-bearing BM-derived cells. To avoid such obstacles, one could envision a regional application of selectively targeted agonists or modulators through peri- or intravascular routes. This may be accomplished using polymer- or nanoparticle-based delivery, as exemplified for microR-126-3p, which specifically derepresses CXCR4 activity in ECs.[10] Likewise, the therapeutic feasibility shown for target site blockers[50] could be extended to blocking specific microRNA interactions with CXCR4.

AUTHORS

Yvonne Döring, PhD*; Heidi Noels, PhD*; Emiel P.C. van der Vorst, PhD†; Carlos Neideck, MSc†; Virginia Egea, PhD; Maik Drechsler, PhD; Manuela Mandl, PhD; Lukas Pawig, PhD; Yvonne Jansen, BS; Katrin Schröder, PhD; Kiril Bidzhekov, PhD; Remco T.A. Megens, PhD; Wendy Theelen, PhD; Barbara M. Klinkhammer, PhD; Peter Boor, MD, PhD; Leon Schurgers, PhD; Rick van Gorp, MSc; Christian Ries, PhD; Pascal J.H. Kusters, MSc; Allard van der Wal, MD, PhD; Tilman M. Hackeng, PhD; Gabor Gäbel, MD; Ralf P. Brandes, MD; Oliver Soehnlein, MD, PhD; Esther Lutgens, MD, PhD; Dietmar Vestweber, PhD; Daniel Teupser, MD; Lesca M. Holdt, MD; PhD; Daniel J. Rader, MD; Danish Saleheen, MD; Christian Weber, MD

ACKNOWLEDGMENTS

We thank Y. Zou (Columbia University, New York), R.H. Adams (University of Münster, Germany), S. Offermanns (University of Heidelberg, Germany) for providing *Cxcr4*^{flox}, Bmx-CreER^{T2}, and Smmhc-CreER^{T2} mice, respectively, and J. Jankowski for support with housing. We thank M. Garbe, S. Elbin, R. Soltan, N. Persigehl, and B. Zhou for excellent technical assistance. Author contributions are as follows: Drs Döring and Noels designed the study, performed mouse and in vitro experiments, analyzed data, and wrote the paper. Drs van der Vorst and Megens performed and analyzed the in vivo experiments. Dr Egea performed luciferase assays, immunoblots, and quantitative real-time polymerase chain reaction. Dr Drechsler performed in vivo permeability studies. Drs Mandl and Neideck performed mouse experiments, collected and processed the histological data, performed flow cytometry analysis and in vivo permeability studies. Dr Pawig performed immunoblots, quantitative real-time polymerase chain reaction, and in vitro permeability assays and processed histological data. Y. Jansen performed atherosclerotic plaque analysis and immunohistochemistry. Dr Schröder and Brandes performed and analyzed vascular reactivity studies. Drs Bidzhekov and Ries contributed to vector design and construction. Dr Theelen performed flow cytometry analysis and analyzed quantitative real-time polymerase chain reaction data. Drs Klinkhammer and Boor performed blood pressure measurements. Drs Schurgers, van Gorp, and Hackeng performed in vitro experiments and contributed critical reagents. Drs Kusters, van der Wal, and Lutgens performed and analyzed human plaque immunohistochemistry. Drs Gäbel, Teupser, and Holdt performed and analyzed human endarterectomy studies. Dr Soehnlein performed and analyzed intravital microscopy experiments. Vestweber contributed a critical mouse model. Dr Rader was involved in study design and contributed to lipid uptake experiments. Dr Saleheen performed and analyzed genome-wide association studies. Dr Weber designed and supervised the study, analyzed data, and wrote the paper. All authors discussed the results and commented on the manuscript.

SOURCES OF FUNDING

This work was funded by Deutsche Forschungsgemeinschaft (SFB1123-A1 to Drs Weber and Döring and SFB1123-Z1 to Dr Megens), National Institutes of Health (1R01HL122843 to Drs Saleheen, Rader, and Weber), the Fondation Leducq Transatlantic Network of Excellence CVGeneF(x) to Drs Weber and Rader, the German Federal Ministry of Education and Research (01KU1213A to Dr Weber), the European Research Council (ERC Advanced Grant 692511 to Dr Weber), the German Center for Cardiovascular Research (MHA VD1.2, 81Z1600212, and 81X2800151 to Drs Weber, Soehnlein, Döring, Noels, and Brandes), the German Heart Foundation (F/40/12 to Dr Noels), the START-program (49/13 to Dr Noels) and the Habilitation program of the Faculty of Medicine, RWTH Aachen (to Dr Noels).

DISCLOSURES

None.

AFFILIATIONS

From Institute for Cardiovascular Prevention (IPEK), LMU Munich, Germany (Y.D., E.P.C.v.d.V., C.N., V.E., M.D., M.M., Y.J., K.B., R.T.A.M., C.R., O.S., E.T., C.W.); Institute for Molecular Cardiovascular Research (IMCAR), RWTH Aachen University, Germany (H.N., L.P., W.T.); Institute for Cardiovascular Physiology, Vascular Research Centre, Goethe University, Frankfurt am Main, Germany (K.S., R.P.B.); Division of Nephrology and Immunology, RWTH Aachen University Hospital, Germany (B.M.K., P.B.); Cardiovascular Research Institute Maastricht (CARIM), Department of Biochemistry, Maastricht University, the Netherlands (R.T.A.M., R.v.G., T.M.H., C.W.); Academic Medical Center, Department of Pathology and Department of Medical Biochemistry, Amsterdam University, the Netherlands (P.J.H.K., A.v.D.W., E.T.); Department of Vascular and Endovascular Surgery, LMU Munich, Germany (G.G.); DZHK (German Centre for

Cardiovascular Research), partner site Frankfurt am Main, Germany (R.P.B.); DZHK (German Centre for Cardiovascular Research), partner site Munich Heart Alliance, Germany (O.S., C.W.); Department of Physiology and Pharmacology, Karolinksa Institutet, Stockholm, Sweden (O.S.); Max-Plank-Institute for Molecular Biomedicine, Münster, Germany (D.V.); Institute for Laboratory Medicine, LMU Munich, Germany (D.T., L.M.H.); and Division of Translational Medicine and Human Genetics, Department of Medicine, Perelman School of Medicine at the University of Pennsylvania, Philadelphia, PA (D.J.R., D.S.).

FOOTNOTES

Received January 30, 2017; accepted April 17, 2017.

The online-only Data Supplement is available with this article at http://circ.ahajournals.org/lookup/suppl/doi:10.1161/CIRCULATIONAHA.117.027646/-/DC1.

Circulation is available at http://circ.ahajournals.org.

REFERENCES

1. Döring Y, Pawig L, Weber C, Noels H. The CXCL12/CXCR4 chemokine ligand/receptor axis in cardiovascular disease. *Front Physiol*. 2014;5:212. doi: 10.3389/fphys.2014.00212.
2. Zou YR, Kottmann AH, Kuroda M, Taniuchi I, Littman DR. Function of the chemokine receptor CXCR4 in haematopoiesis and in cerebellar development. *Nature*. 1998;393:595–599. doi: 10.1038/31269.
3. Tachibana K, Hirota S, Iizasa H, Yoshida H, Kawabata K, Kataoka Y, Kitamura Y, Matsushima K, Yoshida N, Nishikawa S, Kishimoto T, Nagasawa T. The chemokine receptor CXCR4 is essential for vascularization of the gastrointestinal tract. *Nature*. 1998;393:591–594. doi: 10.1038/31261.
4. Nagasawa T, Hirota S, Tachibana K, Takakura N, Nishikawa S, Kitamura Y, Yoshida N, Kikutani H, Kishimoto T. Defects of B-cell lymphopoiesis and bone-marrow myelopoiesis in mice lacking the CXC chemokine PBSF/SDF-1. *Nature*. 1996;382:635–638. doi: 10.1038/382635a0.
5. Zernecke A, Schober A, Bot I, von Hundelshausen P, Liehn EA, Möpps B, Mericskay M, Gierschik P, Biessen EA, Weber C. SDF-1alpha/CXCR4 axis is instrumental in neointimal hyperplasia and recruitment of smooth muscle progenitor cells. *Circ Res*. 2005;96:784–791. doi: 10.1161/01.RES.0000162100.52009.38.
6. Weber C, Noels H. Atherosclerosis: current pathogenesis and therapeutic options. *Nat Med*. 2011;17:1410–1422. doi: 10.1038/nm.2538.
7. Noels H, Zhou B, Tilstam PV, Theelen W, Li X, Pawig L, Schmitz C, Akhtar S, Simsekyilmaz S, Shagdarsuren E, Schober A, Adams RH, Bernhagen J, Liehn EA, Döring Y, Weber C. Deficiency of endothelial CXCR4 reduces reendothelialization and enhances neointimal hyperplasia after vascular injury in atherosclerosis-prone mice. *Arterioscler Thromb Vasc Biol*. 2014;34:1209–1220. doi: 10.1161/ATVBAHA.113.302878.
8. Zernecke A, Bot I, Djalali-Talab Y, Shagdarsuren E, Bidzhekov K, Meiler S, Krohn R, Schober A, Sperandio M, Soehnlein O, Bornemann J, Tacke F, Biessen EA, Weber C. Protective role of CXC receptor 4/CXC ligand 12 unveils the importance of neutrophils in atherosclerosis. *Circ Res*. 2008;102:209–217. doi: 10.1161/CIRCRESAHA.107.160697.
9. Bot I, Daissormont IT, Zernecke A, van Puijvelde GH, Kramp B, de Jager SC, Sluimer JC, Manca M, Hérias V, Westra MM, Bot M, van Santbrink PJ, van Berkel TJ, Su L, Skjelland M, Gullestad L, Kuiper J, Halvorsen B, Aukrust P, Koenen RR, Weber C, Biessen EA. CXCR4 blockade induces atherosclerosis by affecting neutrophil function. *J Mol Cell Cardiol*. 2014;74:44–52. doi: 10.1016/j.yjmcc.2014.04.021.
10. Zernecke A, Bidzhekov K, Noels H, Shagdarsuren E, Gan L, Denecke B, Hristov M, Köppel T, Jahantigh MN, Lutgens E, Wang S, Olson EN, Schober A, Weber C. Delivery of microRNA-126 by apoptotic bodies induces CXCL12-dependent vascular protection. *Sci Signal*. 2009;2:ra81. doi: 10.1126/scisignal.2000610.
11. Samani NJ, Erdmann J, Hall AS, Hengstenberg C, Mangino M, Mayer B, Dixon RJ, Meitinger T, Braund P, Wichmann HE, Barrett JH, König IR, Stevens SE, Szymczak S, Tregouet DA, Iles MM, Pahlke F, Pollard H, Lieb W, Cambien F, Fischer M, Ouwehand W, Blankenberg S, Balmforth AJ, Baessler A, Ball SG, Strom TM, Braenne I, Gieger C, Deloukas P, Tobin MD, Ziegler A, Thompson JR, Schunkert H; WTCCC and the Cardiogenics Consortium. Genomewide association analysis of coronary artery disease. *N Engl J Med*. 2007;357:443–453. doi: 10.1056/NEJMoa072366.
12. Kathiresan S, Voight BF, Purcell S, Musunuru K, Ardissino D, Mannucci PM, Anand S, Engert JC, Samani NJ, Schunkert H, Erdmann J, Reilly MP, Rader DJ, Morgan T, Spertus JA, Stoll M, Girelli D, McKeown PP, Patterson CC, Siscovick DS, O'Donnell CJ, Elosua R, Peltonen L, Salomaa V, Schwartz SM, Melander O, Altshuler D, Ardissino D, Merlini PA, Berzuini C, Bernardinelli L, Peyvandi F, Tubaro M, Celli P, Ferrario M, Fetiveau R, Marziliano N, Casari G, Galli M, Ribichini F, Rossi M, Bernardi F, Zonzin P, Piazza A, Mannucci PM, Schwartz SM, Siscovick DS, Yee J, Friedlander Y, Elosua R, Marrugat J, Lucas G, Subirana I, Sala J, Ramos R, Kathiresan S, Meigs JB, Williams G, Nathan DM, MacRae CA, O'Donnell CJ, Salomaa V, Havulinna AS, Peltonen L, Melander O, Berglund G, Voight BF, Kathiresan S, Hirschhorn JN, Asselta R, Duga S, Spreafico M, Musunuru K, Daly MJ, Purcell S, Voight BF, Purcell S, Nemesh J, Korn JM, McCarroll SA, Schwartz SM, Yee J, Kathiresan S, Lucas G, Subirana I, Elosua R, Surti A, Guiducci C, Gianniny L, Mirel D, Parkin M, Burtt N, Gabriel SB, Samani NJ, Thompson JR, Braund PS, Wright BJ, Balmforth AJ, Ball SG, Hall AS, Schunkert H, Erdmann J, Linsel-Nitschke P, Lieb W, Ziegler A, Konig I, Hengstenberg C, Fischer M, Stark K, Grosshennig A, Preuss M, Wichmann HE, Schreiber S, Schunkert H, Samani NJ, Erdmann J, Ouwehand W, Hengstenberg C, Deloukas P, Scholz M, Cambien F, Reilly MP, Li M, Chen Z, Wilensky R, Matthai W, Qasim A, Hakonarson HH, Devaney J, Burnett MS, Pichard AD, Kent KM, Satler L, Lindsay JM, Waksman R, Knouff CW, Waterworth DM, Walker MC, Mooser V, Epstein SE, Rader DJ, Scheffold T, Berger K, Stoll M, Huge A, Girelli D, Martinelli N, Olivieri O, Corrocher R, Morgan T, Spertus JA, McKeown P, Patterson CC, Schunkert H, Erdmann E, Linsel-Nitschke P, Lieb W, Ziegler A, Konig IR, Hengstenberg C, Fischer M, Stark K, Grosshennig A, Preuss M, Wichmann HE, Schreiber S, Holm H, Thorleifsson G, Thorsteinsdottir U, Stefansson K, Engert JC, Do R, Xie C, Anand S, Kathiresan S, Ardissino D, Mannucci PM, Siscovick D, O'Donnell CJ, Samani NJ, Melander O, Elosua R, Peltonen L, Salomaa V, Schwartz SM, Altshuler D. Genome-wide association of early-onset myocardial infarction with single nucleotide polymorphisms and copy number variants. *Nat Genet*. 2009;41:334–341.
13. Teslovich TM, Musunuru K, Smith AV, Edmondson AC, Stylianou IM, Koseki M, Pirruccello JP, Ripatti S, Chasman DI, Willer CJ, Johansen CT, Fouchier SW, Isaacs A, Peloso GM, Barbalic M, Ricketts SL, Bis JC, Aulchenko YS, Thorleifsson G, Feitosa MF, Chambers J, Orho-Melander M, Melander O, Johnson T, Li X, Guo X, Li M, Shin Cho Y, Jin Go M, Jin Kim Y, Lee JY, Park T, Kim K, Sim X, Twee-Hee Ong R, Croteau-Chonka DC, Lange LA, Smith JD, Song K, Hua Zhao J, Yuan X, Luan J, Lamina C, Ziegler A, Zhang W, Zee RY, Wright AF, Witteman JC, Wilson JF, Willemsen G, Wichmann HE, Whitfield JB, Waterworth DM, Wareham NJ, Waeber G, Vollenweider P, Voight BF, Vitart V, Uitterlinden AG, Uda M, Tuomilehto J, Thompson JR, Tanaka T, Surakka I, Stringham HM, Spector TD, Soranzo N, Smit JH, Sinisalo J, Silander K, Sijbrands EJ, Scuteri A, Scott J, Schlessinger D, Sanna S, Salomaa V, Saharinen J, Sabatti C, Ruokonen A, Rudan I, Rose LM, Roberts R, Rieder M, Psaty BM, Pramstaller PP, Pichler I, Perola M, Penninx BW, Pedersen NL, Pattaro C, Parker AN, Pare G, Oostra BA, O'Donnell CJ, Nieminen MS, Nickerson DA, Montgomery GW, Meitinger T, McPherson R, McCarthy MI, McArdle W, Masson D, Martin NG, Marroni F, Mangino M, Magnusson PK, Lucas G, Luben R, Loos RJ, Lokki ML, Lettre G, Langenberg C, Launer LJ, Lakatta EG, Laaksonen R, Kyvik KO, Kronenberg F, König IR, Khaw KT, Kaprio J, Kaplan LM, Johansson A, Jarvelin MR, Janssens AC, Ingelsson E, Igl W, Kees Hovingh G, Hottenga JJ, Hofman A, Hicks AA, Hengstenberg C, Heid IM, Hayward C, Havulinna AS, Hastie ND, Harris TB, Haritunians T, Hall AS, Gyllensten U, Guiducci C, Groop LC, Gonzalez E, Gieger C, Freimer NB, Ferrucci L, Erdmann J, Elliott P, Ejebe KG, Döring A, Dominiczak AF, Demissie S, Deloukas P, de Geus EJ, de Faire U, Crawford G, Collins FS, Chen YD, Caulfield MJ, Campbell H, Burtt NP, Bonnycastle LL, Boomsma DI, Boekholdt SM, Bergman RN, Barroso I, Bandinelli S, Ballantyne CM, Assimes TL, Quertermous T, Altshuler D, Seielstad M, Wong TY, Tai ES, Feranil AB, Kuzawa CW, Adair LS, Taylor HA Jr, Borecki IB, Gabriel SB, Wilson JG, Holm H, Thorsteinsdottir U, Gudnason V, Krauss RM, Mohlke KL, Ordovas JM, Munroe PB, Kooner JS, Tall AR, Hegele RA, Kastelein JJ, Schadt EE, Rotter JI, Boerwinkle E, Strachan DP, Mooser V, Stefansson K, Reilly MP, Samani NJ, Schunkert H, Cupples LA, Sandhu MS, Ridker PM, Rader DJ, van Duijn CM, Peltonen L, Abecasis GR, Boehnke M, Kathiresan S. Biological, clinical and population relevance of 95 loci for blood lipids. *Nature*. 2010;466:707–713. doi: 10.1038/nature09270.
14. Schober A, Knarren S, Lietz M, Lin EA, Weber C. Crucial role of stromal cell-derived factor-1alpha in neointima formation after vascular injury in

apolipoprotein E-deficient mice. *Circulation*. 2003;108:2491–2497. doi: 10.1161/01.CIR.0000099508.76665.9A.
15. Zoll J, Fontaine V, Gourdy P, Barateau V, Vilar J, Leroyer A, Lopes-Kam I, Mallat Z, Arnal JF, Henry P, Tobelem G, Tedgui A. Role of human smooth muscle cell progenitors in atherosclerotic plaque development and composition. *Cardiovasc Res*. 2008;77:471–480. doi: 10.1093/cvr/cvm034.
16. Foteinos G, Hu Y, Xiao Q, Metzler B, Xu Q. Rapid endothelial turnover in atherosclerosis-prone areas coincides with stem cell repair in apolipoprotein E-deficient mice. *Circulation*. 2008;117:1856–1863. doi: 10.1161/CIRCULATIONAHA.107.746008.
17. Holtwick R, Gotthardt M, Skryabin B, Steinmetz M, Potthast R, Zetsche B, Hammer RE, Herz J, Kuhn M. Smooth muscle-selective deletion of guanylyl cyclase-A prevents the acute but not chronic effects of ANP on blood pressure. *Proc Natl Acad Sci USA*. 2002;99:7142–7147. doi: 10.1073/pnas.102650499.
18. Wirth A, Benyó Z, Lukasova M, Leutgeb B, Wettschureck N, Gorbey S, Orsy P, Horváth B, Maser-Gluth C, Greiner E, Lemmer B, Schütz G, Gutkind JS, Offermanns S. G12-G13-LARG-mediated signaling in vascular smooth muscle is required for salt-induced hypertension. *Nat Med*. 2008;14:64–68. doi: 10.1038/nm1666.
19. Dejana E, Tournier-Lasserve E, Weinstein BM. The control of vascular integrity by endothelial cell junctions: molecular basis and pathological implications. *Dev Cell*. 2009;16:209–221. doi: 10.1016/j.devcel.2009.01.004.
20. Davignon J, Ganz P. Role of endothelial dysfunction in atherosclerosis. *Circulation*. 2004;109:III27–32.
21. Reis M, Czupalla CJ, Ziegler N, Devraj K, Zinke J, Seidel S, Heck R, Thom S, Macas J, Bockamp E, Fruttiger M, Taketo MM, Dimmeler S, Plate KH, Liebner S. Endothelial Wnt/β-catenin signaling inhibits glioma angiogenesis and normalizes tumor blood vessels by inducing PDGF-B expression. *J Exp Med*. 2012;209:1611–1627. doi: 10.1084/jem.20111580.
22. Hwang S, Zimmerman NP, Agle KA, Turner JR, Kumar SN, Dwinell MB. E-cadherin is critical for collective sheet migration and is regulated by the chemokine CXCL12 protein during restitution. *J Biol Chem*. 2012;287:22227–22240. doi: 10.1074/jbc.M112.367979.
23. Broermann A, Winderlich M, Block H, Frye M, Rossaint J, Zarbock A, Cagna G, Linnepe R, Schulte D, Nottebaum AF, Vestweber D. Dissociation of VE-PTP from VE-cadherin is required for leukocyte extravasation and for VEGF-induced vascular permeability in vivo. *J Exp Med*. 2011;208:2393–2401. doi: 10.1084/jem.20110525.
24. Timmerman I, Hoogenboezem M, Bennett AM, Geerts D, Hordijk PL, van Buul JD. The tyrosine phosphatase SHP2 regulates recovery of endothelial adherens junctions through control of β-catenin phosphorylation. *Mol Biol Cell*. 2012;23:4212–4225. doi: 10.1091/mbc.E12-01-0038.
25. van Haperen R, de Waard M, van Deel E, Mees B, Kutryk M, van Aken T, Hamming J, Grosveld F, Duncker DJ, de Crom R. Reduction of blood pressure, plasma cholesterol, and atherosclerosis by elevated endothelial nitric oxide. *J Biol Chem*. 2002;277:48803–48807. doi: 10.1074/jbc.M209477200.
26. Ogura M, Hori M, Harada-Shiba M. Association between cholesterol efflux capacity and atherosclerotic cardiovascular disease in patients with familial hypercholesterolemia. *Arterioscler Thromb Vasc Biol*. 2016;36:181–188. doi: 10.1161/ATVBAHA.115.306665.
27. Smith JD, Miyata M, Ginsberg M, Grigaux C, Shmookler E, Plump AS. Cyclic AMP induces apolipoprotein E binding activity and promotes cholesterol efflux from a macrophage cell line to apolipoprotein acceptors. *J Biol Chem*. 1996;271:30647–30655.
28. Bennett MR, Sinha S, Owens GK. Vascular smooth muscle cells in atherosclerosis. *Circ Res*. 2016;118:692–702. doi: 10.1161/CIRCRESAHA.115.306361.
29. Salabei JK, Cummins TD, Singh M, Jones SP, Bhatnagar A, Hill BG. PDGF-mediated autophagy regulates vascular smooth muscle cell phenotype and resistance to oxidative stress. *Biochem J*. 2013;451:375–388. doi: 10.1042/BJ20121344.
30. Naylor AJ, McGettrick HM, Maynard WD, May P, Barone F, Croft AP, Egginton S, Buckley CD. A differential role for CD248 (Endosialin) in PDGF-mediated skeletal muscle angiogenesis. *PLoS One*. 2014;9:e107146. doi: 10.1371/journal.pone.0107146.
31. Hasanov Z, Ruckdeschel T, König C, Mogler C, Kapel SS, Korn C, Spegg C, Eichwald V, Wieland M, Appak S, Augustin HG. Endosialin promotes atherosclerosis through phenotypic remodeling of vascular smooth muscle cells. *Arterioscler Thromb Vasc Biol*. 2017;37:495–505. doi: 10.1161/ATVBAHA.116.308455.
32. Nakamura Y, Patrushev N, Inomata H, Mehta D, Urao N, Kim HW, Razvi M, Kini V, Mahadev K, Goldstein BJ, McKinney R, Fukai T, Ushio-Fukai M. Role of protein tyrosine phosphatase 1B in vascular endothelial growth factor signaling and cell-cell adhesions in endothelial cells. *Circ Res*. 2008;102:1182–1191. doi: 10.1161/CIRCRESAHA.107.167080.
33. Ukropec JA, Hollinger MK, Salva SM, Woolkalis MJ. SHP2 association with VE-cadherin complexes in human endothelial cells is regulated by thrombin. *J Biol Chem*. 2000;275:5983–5986.
34. Gavard J. Endothelial permeability and VE-cadherin: a wacky comradeship. *Cell Adh Migr*. 2014;8:158–164.
35. Paolinelli R, Corada M, Ferrarini L, Devraj K, Artus C, Czupalla CJ, Rudini N, Maddaluno L, Papa E, Engelhardt B, Couraud PO, Liebner S, Dejana E. Wnt activation of immortalized brain endothelial cells as a tool for generating a standardized model of the blood brain barrier *in vitro*. *PLoS One*. 2013;8:e70233. doi: 10.1371/journal.pone.0070233.
36. Mo W, Chen J, Patel A, Zhang L, Chau V, Li Y, Cho W, Lim K, Xu J, Lazar AJ, Creighton CJ, Bolshakov S, McKay RM, Lev D, Le LQ, Parada LF. CXCR4/CXCL12 mediate autocrine cell- cycle progression in NF1-associated malignant peripheral nerve sheath tumors. *Cell*. 2013;152:1077–1090. doi: 10.1016/j.cell.2013.01.053.
37. Liu Z, Habener JF. Stromal cell-derived factor-1 promotes survival of pancreatic beta cells by the stabilisation of beta-catenin and activation of transcription factor 7-like 2 (TCF7L2). *Diabetologia*. 2009;52:1589–1598. doi: 10.1007/s00125-009-1384-x.
38. Kobayashi K, Sato K, Kida T, Omori K, Hori M, Ozaki H, Murata T. Stromal cell-derived factor-1α/C-X-C chemokine receptor type 4 axis promotes endothelial cell barrier integrity via phosphoinositide 3-kinase and Rac1 activation. *Arterioscler Thromb Vasc Biol*. 2014;34:1716–1722. doi: 10.1161/ATVBAHA.114.303890.
39. Guo C, Goodwin AJ, Buie JN, Cook JA, Halushka PV, Argraves K, Zingarelli B, Zhang XK, Wang L, Fan H. A stromal cell-derived factor 1 alpha analogue improves endothelial cell function in lipopolysaccharide-induced acute respiratory distress syndrome. *Mol Med*. 2016;22:115–123.
40. Gelfand BD, Meller J, Pryor AW, Kahn M, Bortz PD, Wamhoff BR, Blackman BR. Hemodynamic activation of beta-catenin and T-cell-specific transcription factor signaling in vascular endothelium regulates fibronectin expression. *Arterioscler Thromb Vasc Biol*. 2011;31:1625–1633. doi: 10.1161/ATVBAHA.111.227827.
41. Choi SE, Jang HJ, Kang Y, Jung JG, Han SJ, Kim HJ, Kim DJ, Lee KW. Atherosclerosis induced by a high-fat diet is alleviated by lithium chloride via reduction of VCAM expression in ApoE-deficient mice. *Vascul Pharmacol*. 2010;53:264–272. doi: 10.1016/j.vph.2010.09.004.
42. Ai Z, Shao J, Wu Y, Yu M, Du J, Shi X, Shi X, Zhang Y, Guo Z. CHIR99021 enhances Klf4 Expression through β-Catenin Signaling and miR-7a Regulation in J1 Mouse Embryonic Stem Cells. *PLoS One*. 2016;11:e0150936. doi: 10.1371/journal.pone.0150936.
43. Cowan CE, Kohler EE, Dugan TA, Mirza MK, Malik AB, Wary KK. Kruppel-like factor-4 transcriptionally regulates VE-cadherin expression and endothelial barrier function. *Circ Res*. 2010;107:959–966. doi: 10.1161/CIRCRESAHA.110.219592.
44. Zhou G, Hamik A, Nayak L, Tian H, Shi H, Lu Y, Sharma N, Liao X, Hale A, Boerboom L, Feaver RE, Gao H, Desai A, Schmaier A, Gerson SL, Wang Y, Atkins GB, Blackman BR, Simon DI, Jain MK. Endothelial Kruppel-like factor 4 protects against atherothrombosis in mice. *J Clin Invest*. 2012;122:4727–4731. doi: 10.1172/JCI66056.
45. Wu CJ, O'Rourke DM, Feng GS, Johnson GR, Wang Q, Greene MI. The tyrosine phosphatase SHP-2 is required for mediating phosphatidylinositol 3-kinase/Akt activation by growth factors. *Oncogene*. 2001;20:6018–6025. doi: 10.1038/sj.onc.1204699.
46. Ackers-Johnson M, Talasila A, Sage AP, Long X, Bot I, Morrell NW, Bennett MR, Miano JM, Sinha S. Myocardin regulates vascular smooth muscle cell inflammatory activation and disease. *Arterioscler Thromb Vasc Biol*. 2015;35:817–828. doi: 10.1161/ATVBAHA.114.305218.
47. Feil S, Fehrenbacher B, Lukowski R, Essmann F, Schulze-Osthoff K, Schaller M, Feil R. Transdifferentiation of vascular smooth muscle cells to macrophage-like cells during atherogenesis. *Circ Res*. 2014;115:662–667. doi: 10.1161/CIRCRESAHA.115.304634.
48. Allahverdian S, Chehroudi AC, McManus BM, Abraham T, Francis GA. Contribution of intimal smooth muscle cells to cholesterol accumulation and macrophage-like cells in human atherosclerosis. *Circulation*. 2014;129:1551–1559. doi: 10.1161/CIRCULATIONAHA.113.005015.
49. Carthy JM, Luo Z, McManus BM. WNT3A induces a contractile and secretory phenotype in cultured vascular smooth muscle cells that is associated with increased gap junction communication. *Lab Invest*. 2012;92:246–255. doi: 10.1038/labinvest.2011.164.
50. Hartmann P, Zhou Z, Natarelli L, Wei Y, Nazari-Jahantigh M, Zhu M, Grommes J, Steffens S, Weber C, Schober A. Endothelial Dicer promotes atherosclerosis and vascular inflammation by miRNA-103-mediated suppression of KLF4. *Nat Commun*. 2016;7:10521. doi: 10.1038/ncomms10521.